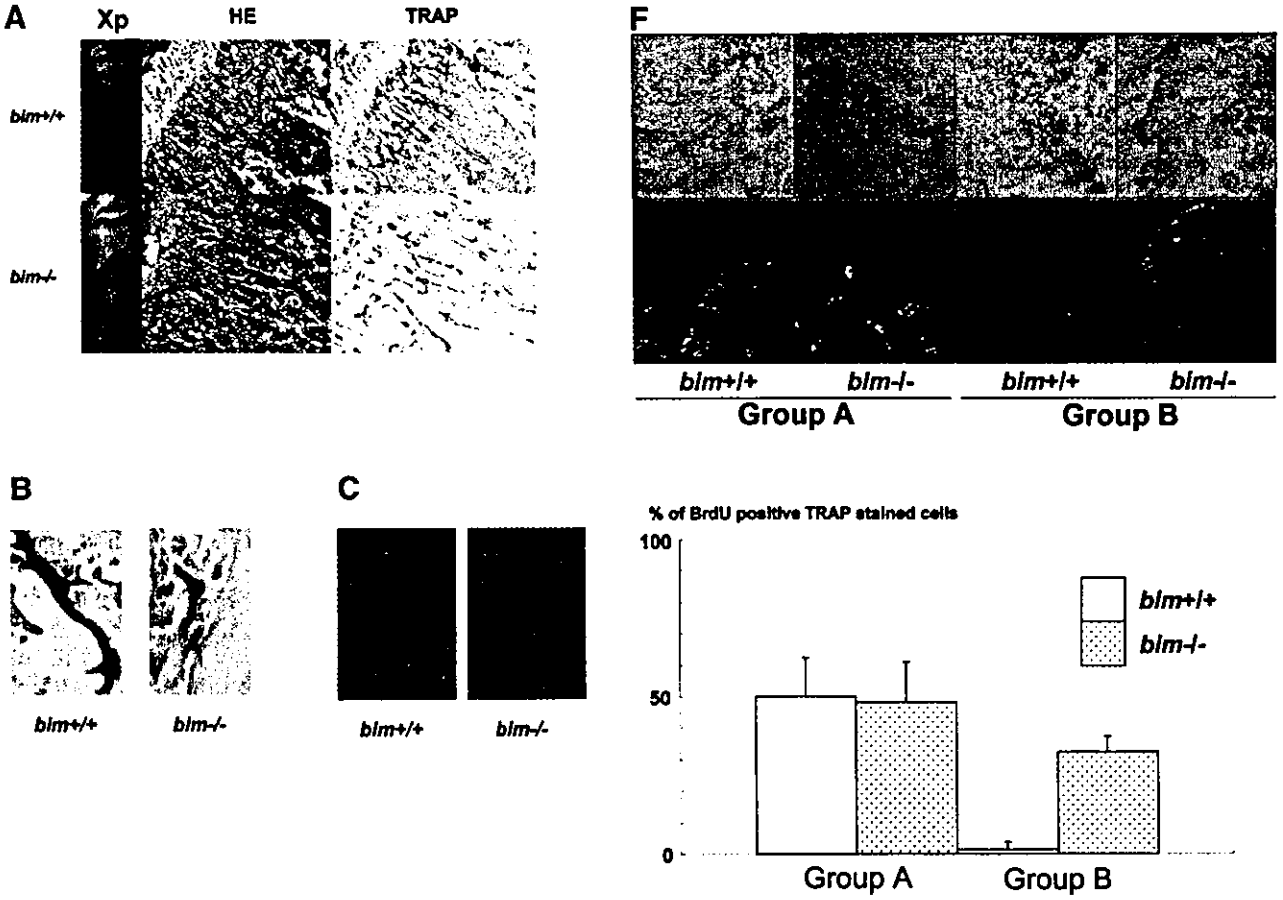

Fig. 3. Bim deficiency causes mild osteosclerosis due to impaired OC activation. (A) Radiological and histological analysis of tibia from 5-week-old *bim+/+* and *bim-/-* male mice (H&E and TRAP staining). *bim-/-* tibia showed expanded secondary spongiosa, exhibiting mild osteosclerosis. (B) *bim-/-* OCs showed smaller and shrunken morphological features compared with *bim+/+* OCs *in vivo* as shown by TRAP staining. (C) Impaired actin ring formation in *bim-/-* OCs. More than 90% of *bim+/+* OCs formed actin rings (left), whereas only 30% of *bim-/-* cells were able to do this (right). (D) Histomorphometric analysis: parameters are measured in the proximal tibia of *bim+/+* and *bim-/-* mice. Data are expressed as means ± SD from five mice of each genotype. BV/TV, trabecular bone volume expressed as a percentage of tibia tissue volume; Tb.Th, trabecular bone thickness; Tb.N, trabecular bone number per mm; Tb.Sp, average space between neighboring trabecular bones; O.Th, osteoid thickness; OS/BS, percentage of bone surface covered by osteoid; Ob.S/BS, percentage of bone surface covered by cuboidal osteoblast; ES/BS, percentage of eroded surface; Oc.N/B.Pm, number of mature OCs per 10 mm of bone perimeter; Oc.S/BS, percentage of bone surface covered by mature OCs. *bim-/-* bones showed reduction of both bone formation markers (O.Th, OS/BS. and Ob.S/BS) and bone resorption markers (ES/BS and Oc.S/BS), and increased Oc.N/B/Pm. *&** = significantly different. *$P < 0.005$, **$P < 0.01$. (E) Calcein double labeling of tibia trabecular bone from 13-week-old *bim+/+* (left) and *bim-/-* mice (right). Labeling is visualized by fluorescent microscopy. (F) *bim-/-* OCs have a longer life span *in vivo*. Five-week-old *bim+/+* and *bim-/-* mice ($n = 4$) were fed with water containing 1 mg/ml BrdU for 1 week (labeling period). Mice were then sacrificed either on the next day (group A) or after 6 weeks (group B) of the labeling period, and their tibias were examined by anti-BrdU immunohistochemistry. More than 100 OCs were examined by BrdU immunostaining in the serial sections of the tibia, and the number of BrdU-positive OCs was counted. Fifty percent of *bim+/+* OCs and 48% of *bim-/-* OCs in group A were positively stained by BrdU. However, the proportion of BrdU-positive OCs was markedly reduced to <5% in group B *bim+/+* mice, due to the apoptotic cell death, while >30% of group B *bim-/-* OCs still exhibited BrdU labeling.

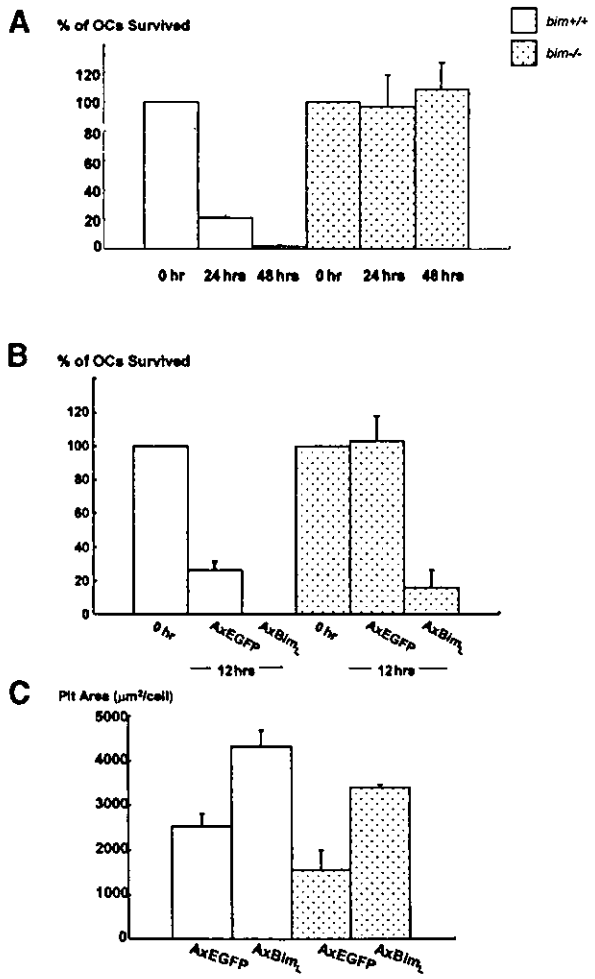

Fig. 4. Effects of Bim on survival and activity of OCs. (A) Survival of *bim+/+* and *bim-/-* OCs. More than 90% of *bim-/-* OCs survived 48 h after M-CSF removal, while all the *bim+/+* OCs had died. (B) Adenovirus vector-mediated Bim_L expression-promoted apoptosis in *bim-/-* OCs as well as in *bim+/+* OCs after 12 h of M-CSF deprivation. (C) Pit-forming activity. The resorption pit area formed by *bim-/-* OCs was significantly less than that formed by *bim+/+* OCs. Overexpression of Bim_L promoted bone-resorbing activity in both *bim+/+* and *bim-/-* OCs.

M-CSF stimulation promotes ubiquitylation-dependent degradation of Bim in OCs

Induction of Bim protein by M-CSF withdrawal (Figure 1A) without changes in mRNA expression levels (Figure 1C) suggested that Bim was regulated post-translationally. Interestingly, treatment of OCs with proteasome inhibitors, such as lactacystin or MG132, greatly enhanced the expression of Bim in OCs even in the presence of M-CSF (Figure 5A). In contrast, MG132 did not affect the expression of other Bcl-2 family members (Figure 5A). This indicates that the ubiquitin–proteasome degradation system is involved in the regulation of Bim expression in these cells. Immunoprecipitation of Bim followed by immunoblot analysis using anti-ubiquitin antibody demonstrated a high level of Bim polyubiquitylation in OCs cultured in MG132, which was greatly enhanced by M-CSF (Figure 5B).

Possible involvement of c-Cbl in ubiquitylation of Bim

The Cbl family proteins are evolutionarily conserved negative regulators of activated tyrosine kinase-coupled receptors, act as E3 ubiquitin ligases, and are involved in OC function (Tanaka *et al.*, 1996; Joazeiro and Weissman, 2000; Sanjay *et al.*, 2001). To determine the role of c-Cbl in the ubiquitylation and degradation of Bim in OCs, we first examined the association of Bim and c-Cbl. GST pull-down experiments showed that recombinant GST–Bim_{EL} fusion protein specifically associated with c-Cbl (Figure 5C, upper panel). c-Cbl was co-immunoprecipitated with Bim in OC lysates in the presence of proteasome inhibitor MG132, and this association was enhanced by M-CSF treatment (Figure 5C, lower panel). Immunofluorescence analysis showed clear co-localization (yellow in Figure 5D, c and d) of Bim and c-Cbl in OCs treated with MG132 and M-CSF. We constructed adenovirus vectors carrying c-Cbl or v-Cbl, which lacks the ubiquitin ligase RING finger domain and acts in a dominant-negative fashion (Taher *et al.*, 2002), and examined their effects on the expression level of Bim in OCs. The upper panel of Figure 5E shows by western blotting with anti-Bim antibody that c-Cbl overexpression (without MG132) reduced Bim expression by increasing Bim ubiquitylation (compare lanes 1 and 5). MG132 treatment increased Bim expression in c-Cbl-overexpressing cells by suppressing proteasomal degradation with or without M-CSF (lanes 7 and 8). In contrast, overexpression of v-Cbl increased the expression of Bim to the maximal level even in the absence of MG132, and the expression was not affected by M-CSF (lanes 9–12). As shown in the lower panel of Figure 5E, overexpression of c-Cbl enhanced Bim ubiquitylation in the absence of M-CSF, and v-Cbl expression suppressed it even in the presence of MG132 and M-CSF.

The role of c-Cbl in M-CSF-dependent ubiquitylation of Bim was confirmed further using OCs generated from c-Cbl-/- mouse bone marrow cells. M-CSF-induced downregulation of Bim was suppressed in c-Cbl-/- OCs as shown by western blotting in Figure 5F. Immunostaining with anti-Bim antibody demonstrated that although no obvious difference in fluorescence intensity was observed between authentic OCs isolated from c-Cbl+/+ and c-Cbl-/- mice, downregulation of Bim by M-CSF treatment was suppressed in c-Cbl-/- OCs (Figure 5G). These results suggest that c-Cbl plays an important role in the ubiquitylation and proteasome-dependent degradation of Bim in OCs.

Stabilization of Bim by lysine mutation reduced the ability of M-CSF to inhibit OC apoptosis

One of the first steps in the ubiquitin–proteasome degradation system includes selective modification of ε-NH_2 groups of lysine residues by ubiquitylation. We constructed retroviral vectors encoding wild-type (wt) or mutated (mt) Bim_{EL}, in which all the ubiquitin acceptor lysine residues (Lys3 and Lys108) are mutated to arginine. These vectors also contained an internal ribosomal entry site (IRES) and enhanced green fluorescent protein (EGFP) to allow identification of infected cells. *bim-/-* OC precursors were infected with either control virus (pMx-IRES-EGFP), pMxBim_{EL}-IRES-EGFP

or pMxmtBim$_{EL}$-IRES-EGFP in the presence of M-CSF and a pan-caspase inhibitor zVAD-FMK. Removal of zVAD-FMK induced rapid apoptosis in the cells expressing mtBimEL within 18 h even in the presence of M-CSF, while almost all of control virus- or 77% of pMx-IRES-Bim$_{EL}$-infected cells survived for at least 24 h. MG132 treatment clearly upregulated the expression of wtBim$_{EL}$, while it did not affect mtBim expression (Figure 6C). Immunoprecipitated mtBim was not ubiquitylated even in the presence of M-CSF and MG132, compared with the wtBim (Figure 6D). These results demonstrate that ubiquitylation and proteasome-mediated degradation are critical regulators of the pro-apoptotic activity of Bim, at least in OCs and their precursors.

Discussion

OCs are terminally differentiated cells with a short life span and, in the absence of trophic factors, such as M-CSF or RANKL, they undergo rapid apoptosis. In the present study, we found that Bim is essential for cytokine withdrawal-induced apoptosis of OCs. Interestingly, although the number of OCs per bone surface was increased and the life span of OCs was elongated in *bim–/–* mice, these animals had mild osteosclerosis due to the low turnover of the skeletal tissues. This phenotype appears to be due to abnormalities in OCs because they are the only relevant cell type in skeletal tissues that express Bim. Moreover, experiments in tissue culture demonstrated that in spite of the retarded apoptosis of *bim–/–* OCs, bone-resorbing activity was significantly reduced compared with *bim+/+* OCs. Adenovirus vector-mediated restoration of Bim$_L$ expression in *bim–/–* OCs not only promoted cytokine withdrawal-induced apoptosis but also upregulated their bone-resorbing activity. Our results are reminiscent of previous studies by Roodman and coworkers, which showed that OC-specific overexpression of Bcl-xL and SV40 large T antigen under the control of TRAP promoter in transgenic mice induced osteosclerosis although OC apoptosis was markedly reduced in the animals (Hentunen *et al.*, 1998). These results suggest that the balance between Bim and anti-apoptotic Bcl-2 family members, such as Bcl-2 and Bcl-xL, is critical for normal skeletal homeostasis. The molecular mechanism of reduced bone-resorbing activity in *bim–/–* OCs still remains unclear. Several previous studies demonstrated that although M-CSF promotes the survival of OCs, it rather suppresses their bone-resorbing activity (Hattersley *et al.*, 1988; Fuller *et al.*, 1993; Miyazaki *et al.*, 2000). M-CSF induces cytoskeletal reorganization of OCs and enhances their migration and chemotaxis, and motile OCs are non-polarized cells with low bone-resorbing activity. Because M-CSF strongly suppressed Bim expression in OCs, we speculate that *bim* deficiency somehow mimics M-CSF treatment, which may explain the reduced bone-resorbing activity of the cells. Alternatively, aged OCs that have already engorged a lot of bone become exhausted, making it difficult to resorb more bone, and the presence of aged OCs suppresses the beginning of the new bone remodeling cycle. Further studies are required to clarify further the molecular mechanism of the reduced bone resorption of *bim–/–* OCs and the osteosclerosis in *bim–/–* mice.

Recently, the role of ubiquitylation in regulating apoptosis has been widely recognized and attracted a great deal of interest (Jesenberger and Jentsch, 2002). For example, p53, which is essential for DNA damage-induced apoptosis in many cell types, is degraded by the ubiquitin–proteasome pathways (Haupt *et al.*, 1997; Kubbutat *et al.*, 1997). Moreover, inhibitor of apoptosis proteins (IAPs) (e.g. XIAP, cIAP1 and cIAP2), which can bind and neutralize initiator and/or effecter caspases, contain RING finger domains, and promote their auto-ubiquitylation and proteasome-mediated degradation when cells are exposed to apoptotic stimuli (Yang *et al.*, 2000). Dephosphorylation and subsequent ubiquitylation-dependent degradation of Bcl-2 was reported to be involved in TNF-α-induced apoptosis of endothelial cells (Dimmeler *et al.*, 1999). Finally, proteasome-dependent degradation of the BH3-only proteins Bid (tBid) and Bik has been reported in HeLa cells and leukemia-derived cells, respectively (Breitschopf *et al.*, 2000; Marshansky *et al.*, 2001). Previous studies have revealed that Bim can be regulated at the transcriptional level in hemopoietic progenitors and neurons (Putcha *et al.*, 2001; Shinjyo *et al.*, 2001; Whitfield *et al.*, 2001; Dijkers *et al.*, 2002), and the regulation of Bim activity by phosphorylation by ERK and/or JNK has been reported (Biswas and Greene, 2002; Lei and Davis, 2003; Weston *et al.*, 2003). Very recently, the ubiquitylation of Bim and its upregulation by proteasome inhibitors were reported (Ley *et al.*, 2003). However, the physiological function of such a modification, especially in primary cells, has not been established. We demonstrate here that Bim ubiquitylation is regulated by M-CSF in OCs, and this modification plays a critical role in their survival. In M-CSF-stimulated cells, Bim is ubiquitylated and its expression kept at low levels by proteasomal degradation. After cytokine withdrawal, Bim protein levels are rapidly increased due to the reduced ubiquitylation and degradation. Bim is associated with c-Cbl in OCs, and overexpression of c-Cbl suppressed the expression of Bim in OCs by promoting its ubiquitylation, while that of v-Cbl, which acts in a dominant-negative fashion, increased the Bim level even in the presence of M-CSF, suggesting the important role of c-Cbl in Bim ubiquitylation. This was confirmed further using OCs from c-Cbl–/– mice (Figure 5F and G).

The critical role of ubiquitylation and proteasome-mediated degradation in regulating the pro-apoptotic activity of Bim was proven by showing that a mutant of Bim$_{EL}$ that cannot be ubiquitylated can kill OCs even in the presence of M-CSF, whereas wtBim$_{EL}$ can be kept in check by cytokine receptor signaling. We found that MEK1^{CA} introduction downregulates Bim expression in OCs, and a specific inhibitor of MEK/ERK pathways, PD98059, abolished the effect of M-CSF (Figure 5B), indicating that ERK signaling mainly promotes Bim ubiquitylation. This suggests that the state of phosphorylation of Bim may be important for its ubiquitylation, or that E3 ubiquitin ligation to Bim is regulated mainly by ERK pathways. The detailed mechanism of Bim ubiquitylation still remains elusive.

Targeted disruption of *bim* induced the accumulation of myeloid and lymphoid cells, and perturbation of T-cell development, and caused autoimmune disorders (Bouillet *et al.*, 1999, 2002; Villunger *et al.*, 2003). Bim is also

involved in the apoptosis of neurons (Putcha *et al.*, 2001; Whitfield *et al.*, 2001), and we found that it plays an essential role in regulating the survival and bone-resorbing activity of OCs. There is substantial evidence that abnormalities in the ubiquitylation/proteasome degradation machinery can cause diseases, such as neurodegenerative diseases, cancers and autoimmune diseases (Glickman and Ciechanover, 2002). Therefore, the failure in the ubiquitin–proteasome-dependent degradation of Bim may cause various abnormalities in the skeletal homeostasis, the immune systems and neuronal systems. Further studies are required to elucidate the mechanism of action and the regulation of Bim, and the role of Bim in skeletal disorders.

Materials and methods

Antibodies and chemicals

Antibodies to Bid and Bax were purchased from Cell Signaling Technology (Beverly, MA). Antibodies to Bim (M-20 for immunoprecipitation), Bcl-xL, ubiquitin and c-Cbl were from Santa Cruz Technology (Santa Cruz, CA), and antibodies to Bim (for western blotting) were from BD Biosciences Pharmingen (San Jose, CA). Antibody to Bim (for immunocytochemistry) was from Oncogene Research Products (Cambridge, MA). Recombinant mouse M-CSF was

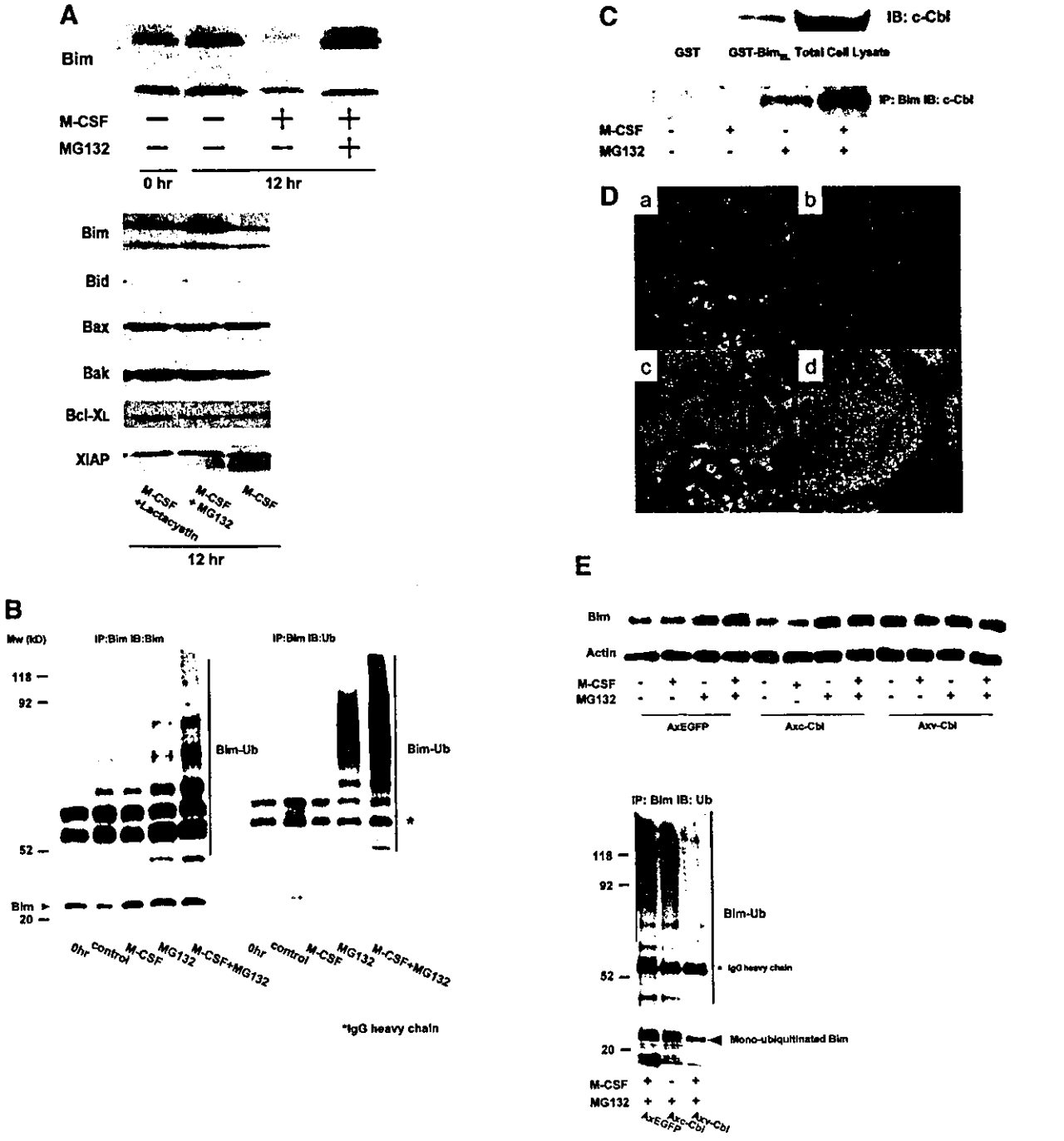

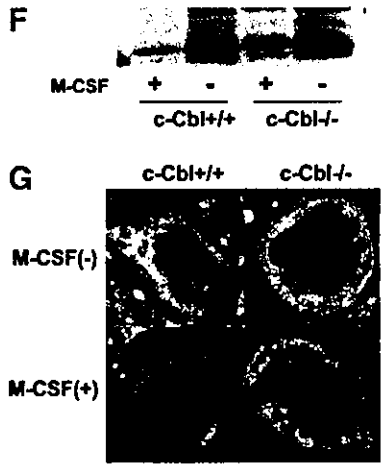

Fig. 5. Ubiquitylation-dependent degradation of Bim in OCs. (A) Western blotting. Upper panel: Bim protein level increased after 12 h of osteoblast removal, which was suppressed in the presence of M-CSF. MG132 treatment strongly upregulated Bim expression even in the presence of M-CSF. Lower panel: no obvious upregulation or downregulation of Bid, Bax, Bak, Bcl-xL and XIAP level was induced by MG132 or lactacystin. (B) Ubiquitylation of Bim in OCs. Proteins immunoprecipitated with anti-Bim antibody were immunoblotted with an anti-Bim antibody (left) or an anti-ubiquitin antibody (right). Ubiquitylated Bim was detected as upper-shifted bands in both anti-Bim and anti-ubiquitin blotting (Bim-Ub). Ubiquitylated Bim was detected when cells were treated with MG132, and marked enhancement of its ubiquitylation was induced by M-CSF treatment. (C) Association of c-Cbl with Bim in OCs. Upper panel: cell lysates of M-CSF-treated OCs were incubated with bacterially expressed GST-Bim_{EL} fusion protein, and association with c-Cbl was determined by western blotting. c-Cbl was associated with GST-Bim_{EL} but not with GST. Lower panel: Bim was immunoprecipitated from OC cell lysates, and its association with c-Cbl was examined by western blotting. Co-immunoprecipitation of c-Cbl with Bim was observed in MG132-treated OCs, which was enhanced by M-CSF treatment. (D) Double immunofluorescence of (a) Bim (green) and (b) c-Cbl (red) in authentic OCs isolated from normal mice. Co-localization of these two molecules (yellow in c and d) was observed in the presence of MG132 and M-CSF. (d) An enlargement of the rectangular area in (c). (E) Involvement of c-Cbl in the ubiquitylation of Bim in OCs. Upper panel: adenovirus vector-mediated overexpression of c-Cbl (Axc-Cbl) decreased the protein level of Bim in OCs in the absence of M-CSF (compare lanes 1 and 5). MG132 treatment increased Bim expression in c-Cbl-overexpressing cells with or without M-CSF (lanes 7 and 8). On the other hand, adenovirus vector-induced overexpression of v-Cbl (Axv-Cbl) increased Bim expression even in the absence of MG132, which was not affected by M-CSF treatment (lanes 9–12). Lower panel: Bim was immunoprecipitated and immunoblotted with anti-ubiquitin antibody. c-Cbl-overexpressing OCs showed Bim ubiquitylation in the absence of M-CSF (lane 2) to a similar extent as in EGFP virus-infected OCs treated with M-CSF (lane 1). v-Cbl overexpression suppressed Bim ubiquitylation even in the presence of MG132 and M-CSF (lane 3). (F) M-CSF-induced downregulation of Bim was suppressed in c-Cbl–/– OCs. OCs generated from bone marrow cells of c-Cbl–/– mice (c-Cbl–/–) or their normal littermates (c-Cbl+/+) were treated or not with M-CSF. Western blotting with anti-Bim antibody demonstrates that although no difference in Bim level was observed between c-Cbl+/+ and c-Cbl–/– OCs in the absence of M-CSF (lanes 2 and 4, respectively), M-CSF-induced downregulation of Bim was suppressed in c-Cbl–/– OCs (lane 3). (G) Immunofluorescence of primary OCs with anti-Bim antibody. Primary OCs isolated from c-Cbl+/+ and c-Cbl–/– mice were cultured in the presence or absence of M-CSF (10 ng/ml) for 12 h, and immunostained with anti-Bim antibody. Although no apparent difference in fluorescence intensity was observed between c-Cbl+/+ and c-Cbl–/– OCs in the absence of M-CSF, M-CSF-induced downregulation was scarcely detected in c-Cbl–/– OCs.

bought from TECHNE Co. (Minneapolis, MN) and soluble RANKL was from Wako Pure Chemical Co. (Osaka, Japan). α-Modified minimum essential medium (αMEM) was purchased from Gibco-BRL, Life Technologies Inc. (Rockville, MD), and fetal bovine serum (FBS) was from Sigma (St Louis, MO). Bacterial collagenase was purchased from Wako Pure Chemical Co. (Osaka, Japan), $1\alpha,25(OH)_2D_3$ from Calbiochem (La Jolla, CA) and dispase from Godoshusei (Tokyo, Japan). The broad-spectrum caspase inhibitor zVAD-FMK was from Calbiochem. Other chemicals and reagents used in this study were of analytical grade.

Expression constructs and gene transduction

The recombinant adenovirus vectors were constructed as previously described (Miyazaki *et al.*, 2000; Mochizuki *et al.*, 2002; Yamaguchi *et al.*, 2003). Adenovirus infection of OCs was performed as previously reported (Tanaka *et al.*, 1998; Miyazaki *et al.*, 2003). Retroviral vectors, pMx-Bim_{EL}-IRES-EGFP and pMx-mtBim_{EL}-IRES-EGFP, were constructed by inserting full-length mouse cDNA of bim_{EL} and mutated bim_{EL}, in which the two ubiquitin acceptor lysine residues (Lys3 and Lys108) were mutated to arginine, into pMx-IRES-EGFP vector. Retrovirus packaging was performed by transfection of the pMx vectors into BOSC cells. Retrovirus infection of OC precursors was carried out as previously described (Kobayashi *et al.*, 2001).

Animals, cells and cultures

Newborn and 8-week-old male ddY mice were purchased from Shizuoka Laboratories Animal Center (Shizuoka, Japan). The breeding and genotyping of *bim–/–* mice (on a C57BL/6 N>12 genetic background) was performed as previously described (Bouillet *et al.*, 1999). The transgenic mice in which a reporter *lacZ* gene was introduced into the *bim* locus was generated by homologous recombination. c-Cbl–/– mice were generated and identified as previously reported (Naramura *et al.*, 1998). Authentic OCs were obtained from the long bones of 2- to 4-day-old neonatal mice as reported (Chiusaroli *et al.*, 2003). To obtain large numbers of cells for biochemical analyses, we utilized the co-culture system established by Takahashi *et al.* (1988).

Immunoblotting and immunoprecipitation

Immunoblotting and immunoprecipitation were performed as previously reported (Tanaka *et al.*, 1998).

Immunofluorescence

Cells cultured on glass coverslips were fixed in 3.7% (v/v) formaldehyde in phosphate-buffered saline (PBS) for 10 min, and then washed three times in PBS. Cells were permeabilized in 0.05% saponin for 30 min, blocked in 5% normal goat serum (Boehringer) for 30 min, incubated in appropriate primary antibodies, washed in PBS, incubated with fluorescein-conjugated secondary antibody, and finally washed in PBS and mounted in FluorSave. Cells were examined using a confocal imaging system (MRC-600; Bio-Rad Laboratories).

GST fusion proteins

A pGEX plasmid containing the GST-Bim_{EL} was used to transform *Escherichia coli* B21 cells (Life Technologies, Inc.). After induction of protein expression with 0.1 μM isopropyl-1-thio-β-D-galactopyranoside (Sigma) for 2–4 h, the bacteria were resuspended in a lysis buffer containing 50 mM Tris-HCl, pH 8.0, 100 μM NaCl, 1 mM phenylmethylsulfonyl fluoride (PMSF) and 1% Triton X-100 and were disrupted further by sonication. Following centrifugation at 10 000 *g* for 20 min, the induced proteins were adsorbed to bead-immobilized glutathione. Soluble GST fusion proteins were obtained by elution with 2 mM reduced glutathione in 50 mM Tris-HCl pH 8.0. For *in vitro* binding assays, bead-adsorbed GST or GST fusion proteins (5 μg/sample) were incubated with OC cell lysates at 4°C on a rotator for 3 h. The beads were then washed three times with lysis buffer, and bound proteins were subjected to SDS-PAGE under reducing conditions followed by immunoblotting.

RT-PCR and real-time PCR

mRNAs was isolated from OCs, and reverse-transcribed by the Super Script First-Strand Synthesis system for RT-PCR (Invitrogen), according to the manufacturer's protocol. The primers we utilized to detect *bim* and *gapdh* were as follows: *bim*, 5′-ATGGCCAAGCAACCTTCTGA and 3′-TCAATGCCTTCTCCATACCAG; *gapdh*, 5′-GTATGTCGTGGAGT-CTACTGGTGT and 3′-TACTCCTTGGAGGCCATGTAGGCC. The primers utilized to detect *bax* and *bcl-xL* were as previously reported by Okahashi *et al.* (1998). Reverse-transcribed mRNAs were analyzed by the ABI Prism® 7000 Sequence Detection System (Applied Biosystems,

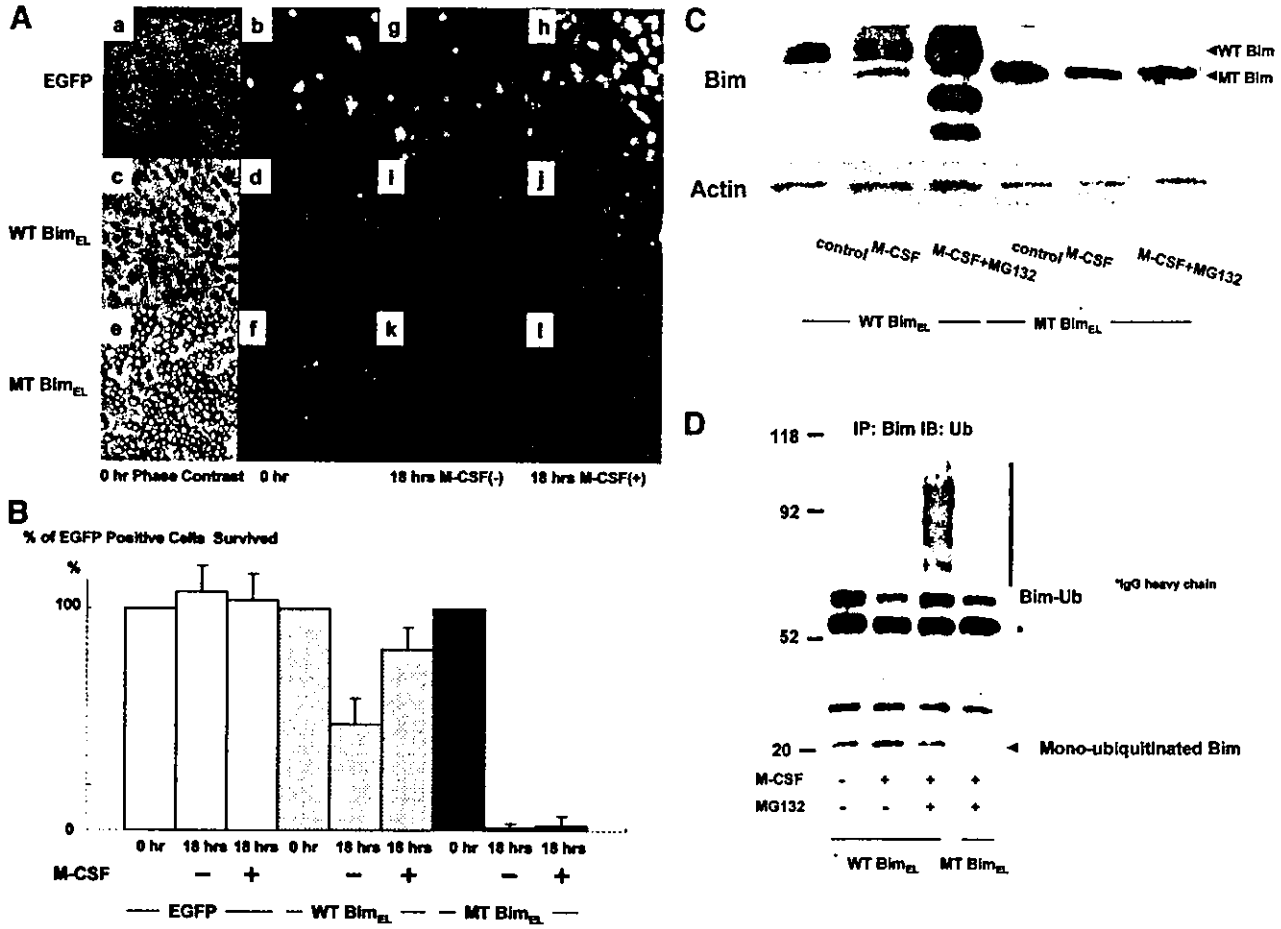

Fig. 6. Effect of mutations in Bim that prevent ubiquitylation. (A) Phase contrast (a, c and e) and immunofluorescence microscopy: *bim–/–* bone marrow cells cultured in the presence of M-CSF (100 ng/ml) and zVAD-FMK (100 μM) were infected with either pMx-IRES-EGFP, pMxBim$_{EL}$-IRES-EGFP or pMxmtBim$_{EL}$-IRES-EGFP. After 7 days of the retrovirus infection, when gene expression was confirmed by EGFP fluorescence (b, d and f), cultures were deprived of zVAD-FMK. At 18 h after zVAD-FMK removal, most of pMx-IRES-EGFP- and pMxBim$_{EL}$-IRES-EGFP-infected cells survived as identified by EGFP fluorescence (h and j), compared with the survival rate of 5% in pMxmtBim$_{EL}$-IRES-EGFP virus-infected cells (l). Both pMxBim$_{EL}$-IRES-EGFP- and pMxmtBim$_{EL}$-IRES-EGFP-infected cells died when M-CSF was removed from the cultures (i and k). (B) The survival ratio of EGFP-positive cells. Almost 100% of the control cells survived even 18 h after z-VAD-FMK removal in the presence of M-CSF. At 18 h after zVAD-FMK removal, almost 100% of pMx-IRES-EGFP- and >70% of pMxBim$_{EL}$-IRES-EGFP-infected cells survived as identified by EGFP fluorescence (EGFP and WTBim$_{EL}$), compared with the survival rate of 5% in pMxmtBim$_{EL}$-IRES-EGFP virus-infected cells (MTBim$_{EL}$). (C) The proteasome inhibitor MG132 enhanced the expression level of wtBim in pMxBim$_{EL}$-IRES-EGFP-infected OC precursors (WTBim) even in the presence of M-CSF, while no obvious upregulation of MTBim was observed in pMxmtBim$_{EL}$-IRES-EGFP infected cells (MTBim). (D) WTBim or MTBim was immunoprecipitated from cell lysates of pMxBim$_{EL}$-IRES-EGFP-infected (WTBim$_{EL}$) or pMxmtBim$_{EL}$-IRES-EGFP-infected cells (MTBim$_{EL}$) using anti-Bim polyclonal antibody, and the immunoprecipitates were immunoblotted with anti-ubiquitin antibody. Treating the cells with the proteasome inhibitor MG132 strongly increased the ubiquitylation of Bim, while no ubiquitylation of mtBim was observed.

CA). The primers we utilized in real-time PCR to detect the common form of all *bim* splice variants and the *bim$_{EL}$*-specific form were as follows: *bim* common form, 5′-CTTCCATACGACAGTCTC and 3′-AACCATTTGAGGGTGGTCTTC; *bim$_{EL}$*-specific form, 5′-GTCCTC-CAGTGGGTATTTCT and 3′-CAGATCTTCAGGTTCCTCCT.

In situ hybridization

In situ hybridization was performed as described previously (Lee *et al.*, 1995) by using complementary digoxigenin-labeled riboprobes for mouse *bim$_L$*, procollagen type IA and procollagen type IIA.

Histomorphometry

Histomorphometric analysis of proximal tibia from *bim+/+* and *bim–/–* littermates was performed as previously described (Akune *et al.*, 2002).

Survival of OCs

The survival of OCs was measured as previously reported (Miyazaki *et al.*, 2000). Cell survival is expressed as the percentage of morphologically intact TRAP-positive multinucleated cells. Other cultures were incubated further for the indicated times, and then the number of living OCs was counted. The number of viable cells remaining at the different time points is shown as a percentage of the cells at the start of the experiment.

Pit formation assay

The pit formation assay was performed as previously described (Tanaka *et al.*, 1998). The resorbed area was measured using an image analysis system (SYSTEM SUPPLY, Nagano, Japan) linked to a light microscope (Nikon, Tokyo, Japan).

Statistical analysis

Each series of experiments was repeated at least three times. The results obtained from a typical experiment were expressed as the means ± SD. Significant differences were determined using factorial analysis of variance.

Acknowledgements

The authors thank R.Yamaguchi and M.Ikeuchi (Department of Orthopaedic Surgery, The University of Tokyo), L.Neff (Yale University) and M.Robati (WEHI) for expert technical assistance,

Y.Azuma (Teijin Institute for Biomedical Research) for histomorphometric analysis, A.Asai and T.Kirino (Department of Neurosurgery, The University of Tokyo) for providing Bcl-xL adenovirus, H.Katagiri (Tohoku University) and T.Asano (The University of Tokyo) for MEK^{CA} and myrAKT adenoviruses, T.Kitamura (Institute of Medial Science, The University of Tokyo) for pMx vectors, and J.Adams and S.Cory (WEHI) for *bim–/–* mice. This work was supported by fellowships and Grants-in-Aid from the Ministry of Education, Science, Sports and Culture of Japan, the Health Science Research Grants from the Ministry of Health and Welfare of Japan, Uehara Memorial Award, Nakatomi Health Science Foundation Award, Grants-in-Aid from the Research Society for Metabolic Bone Diseases to S.T., and by the NHMRC (Canberra), the Leukemia and Lymphoma Society of America and the Dr Josef Steiner Cancer Research Foundation (Bern).

References

Akune,T. *et al.* (2002) Insulin receptor substrate-2 maintains predominance of anabolic function over catabolic function of osteoblasts. *J. Cell Biol.*, **159**, 147–156.

Baron,R. (1989) Molecular mechanisms of bone resorption by the osteoclast. *Anat. Rec.*, **224**, 317–324.

Biswas,S.C. and Greene,L.A. (2002) Nerve growth factor (NGF) down-regulates the Bcl-2 homology 3 (BH3) domain-only protein Bim and suppresses its proapoptotic activity by phosphorylation. *J. Biol. Chem.*, **277**, 49511–49516.

Bouillet,P., Metcalf,D., Huang,D.C., Tarlinton,D.M., Kay,T.W., Kontgen,F., Adams,J.M. and Strasser,A. (1999) Proapoptotic Bcl-2 relative Bim required for certain apoptotic responses, leukocyte homeostasis and to preclude autoimmunity. *Science*, **286**, 1735–1738.

Bouillet,P. *et al.* (2002) BH3-only Bcl-2 family member Bim is required for apoptosis of autoreactive thymocytes. *Nature*, **415**, 922–926.

Breitschopf,K., Zeiher,A.M. and Dimmeler,S. (2000) Ubiquitin-mediated degradation of the proapoptotic active form of bid. A functional consequence on apoptosis induction. *J. Biol. Chem.*, **275**, 21648–21652.

Cheng,E.H., Wei,M.C., Weiler,S., Flavell,R.A., Mak,T.W., Lindsten,T. and Korsmeyer,S.J. (2001) BCL-2, BCL-X(L) sequester BH3 domain-only molecules preventing BAX- and BAK-mediated mitochondrial apoptosis. *Mol. Cell*, **8**, 705–711.

Chiusaroli,R., Sanjay,A., Henriksen,K., Engsig,M.T., Horne,W.C., Gu,H. and Baron,R. (2003) Deletion of the gene encoding c-Cbl alters the ability of osteoclasts to migrate, delaying resorption and ossification of cartilage during the development of long bones. *Dev. Biol.*, **261**, 537–547.

Dijkers,P.F., Birkenkamp,K.U., Lam,E.W., Thomas,N.S., Lammers, J.W., Koenderman,L. and Coffer,P.J. (2002) FKHR-L1 can act as a critical effector of cell death induced by cytokine withdrawal: protein kinase B-enhanced cell survival through maintenance of mitochondrial integrity. *J. Cell Biol.*, **156**, 531–542.

Dimmeler,S., Breitschopf,K., Haendeler,J. and Zeiher,A.M. (1999) Dephosphorylation targets Bcl-2 for ubiquitin-dependent degradation: a link between the apoptosome and the proteasome pathway. *J. Exp. Med.*, **189**, 1815–1822.

Fuller,K., Owens,J.M., Jagger,C.J., Wilson,A., Moss,R. and Chambers,T.J. (1993) Macrophage colony-stimulating factor stimulates survival and chemotactic behavior in isolated osteoclasts. *J. Exp. Med.*, **178**, 1733–1744.

Glantschnig,H., Fisher,J.E., Wesolowski,G., Rodan,G.A. and Reszka,A.A. (2003) M-CSF, TNFα and RANK ligand promote osteoclast survival by signaling through mTOR/S6 kinase. *Cell Death Differ.*, **10**, 1165–1177.

Glickman,M.H. and Ciechanover,A. (2002) The ubiquitin–proteasome proteolytic pathway: destruction for the sake of construction. *Physiol. Rev.*, **82**, 373–428.

Gross,A., McDonnell,J.M. and Korsmeyer,S.J. (1999) BCL-2 family members and the mitochondria in apoptosis. *Genes Dev.*, **13**, 1899–1911.

Hattersley,G., Dorey,E., Horton,M.A. and Chambers,T.J. (1988) Human macrophage colony-stimulating factor inhibits bone resorption by osteoclasts disaggregated from rat bone. *J. Cell. Physiol.*, **137**, 199–203.

Haupt,Y., Maya,R., Kazaz,A. and Oren,M. (1997) Mdm2 promotes the rapid degradation of p53. *Nature*, **387**, 296–299.

Hentunen,T.A. *et al.* (1998) Immortalization of osteoclast precursors by targeting Bcl-XL and simian virus 40 large T antigen to the osteoclast lineage in transgenic mice. *J. Clin. Invest.*, **102**, 88–97.

Huang,D.C. and Strasser,A. (2000) BH3-only proteins—essential initiators of apoptotic cell death. *Cell*, **103**, 839–842.

Hughes,D.E., Wright,K.R., Uy,H.L., Sasaki,A., Yoneda,T., Roodman, G.D., Mundy,G.R. and Boyce,B.F. (1995) Bisphosphonates promote apoptosis in murine osteoclasts *in vitro* and *in vivo*. *J. Bone Miner. Res.*, **10**, 1478–1487.

Jesenberger,V. and Jentsch,S. (2002) Deadly encounter: ubiquitin meets apoptosis. *Nature Rev. Mol. Cell. Biol.*, **3**, 112–121.

Joazeiro,C.A. and Weissman,A.M. (2000) RING finger proteins: mediators of ubiquitin ligase activity. *Cell*, **102**, 549–552.

Kerr,J.F., Wyllie,A.H. and Currie,A.R. (1972) Apoptosis: a basic biological phenomenon with wide-ranging implications in tissue kinetics. *Br. J. Cancer*, **26**, 239–257.

Kobayashi,N., Kadono,Y., Naito,A., Matsumoto,K., Yamamoto,T., Tanaka,S. and Inoue,J. (2001) Segregation of TRAF6-mediated signaling pathways clarifies its role in osteoclastogenesis. *EMBO J.*, **20**, 1271–1280.

Kubbutat,M.H., Jones,S.N. and Vousden,K.H. (1997) Regulation of p53 stability by Mdm2. *Nature*, **387**, 299–303.

Lee,K., Deeds,J.D. and Segre,G.V. (1995) Expression of parathyroid hormone-related peptide and its receptor messenger ribonucleic acids during fetal development of rats. *Endocrinology*, **136**, 453–463.

Lei,K. and Davis,R.J. (2003) JNK phosphorylation of Bim-related members of the Bcl2 family induces Bax-dependent apoptosis. *Proc. Natl Acad. Sci. USA*, **100**, 2432–2437.

Ley,R., Balmanno,K., Hadfield,K., Weston,C.R. and Cook,S.J. (2003) Activation of the ERK1/2 signalling pathway promotes phosphorylation and proteasome-dependent degradation of the BH3-only protein Bim. *J. Biol. Chem.*, **278**, 18811–18816.

Marshansky,V., Wang,X., Bertrand,R., Luo,H., Duguid,W., Chinnadurai,G., Kanaan,N., Vu,M.D. and Wu,J. (2001) Proteasomes modulate balance among proapoptotic and antiapoptotic Bcl-2 family members and compromise functioning of the electron transport chain in leukemic cells. *J. Immunol.*, **166**, 3130–3142.

Miyazaki,T. *et al.* (2000) Reciprocal role of ERK and NF-κB pathways in survival and activation of osteoclasts. *J. Cell Biol.*, **148**, 333–342.

Miyazaki,T., Neff,L., Tanaka,S., Horne,W.C. and Baron,R. (2003) Regulation of cytochrome c oxidase activity by c-Src in osteoclasts. *J. Cell Biol.*, **160**, 709–718.

Mochizuki,T. *et al.* (2002) Akt protein kinase inhibits non-apoptotic programmed cell death induced by ceramide. *J. Biol. Chem.*, **277**, 2790–2797.

Naramura,M., Kole,H.K., Hu,R.J. and Gu,H. (1998) Altered thymic positive selection and intracellular signals in Cbl-deficient mice. *Proc. Natl Acad. Sci. USA*, **95**, 15547–15552.

O'Connor,L., Strasser,A., O'Reilly,L.A., Hausmann,G., Adams,J.M., Cory,S. and Huang,D.C. (1998) Bim: a novel member of the Bcl-2 family that promotes apoptosis. *EMBO J.*, **17**, 384–395.

Okahashi,N., Koide,M., Jimi,E., Suda,T. and Nishihara,T. (1998) Caspases (interleukin-1β-converting enzyme family proteases) are involved in the regulation of the survival of osteoclasts. *Bone*, **23**, 33–41.

O'Reilly,L.A., Cullen,L., Visvader,J., Lindeman,G.J., Print,C., Bath, M.L., Huang,D.C. and Strasser,A. (2000) The proapoptotic BH3-only protein bim is expressed in hematopoietic, epithelial, neuronal and germ cells. *Am. J. Pathol.*, **157**, 449–461.

Putcha,G.V., Moulder,K.L., Golden,J.P., Bouillet,P., Adams,J.A., Strasser,A. and Johnson,E.M. (2001) Induction of BIM, a proapoptotic BH3-only BCL-2 family member, is critical for neuronal apoptosis. *Neuron*, **29**, 615–628.

Sanjay,A. *et al.* (2001) Cbl associates with Pyk2 and Src to regulate Src kinase activity, α(v)β(3) integrin-mediated signaling, cell adhesion and osteoclast motility. *J. Cell Biol.*, **152**, 181–195.

Shinjyo,T. *et al.* (2001) Downregulation of Bim, a proapoptotic relative of Bcl-2, is a pivotal step in cytokine-initiated survival signaling in murine hematopoietic progenitors. *Mol. Cell. Biol.*, **21**, 854–864.

Strasser,A., Harris,A.W., Huang,D.C., Krammer,P.H. and Cory,S. (1995) Bcl-2 and Fas/APO-1 regulate distinct pathways to lymphocyte apoptosis. *EMBO J.*, **14**, 6136–6147.

Strasser,A., O'Connor,L. and Dixit,V.M. (2000) Apoptosis signaling. *Annu. Rev. Biochem.*, **69**, 217–245.

Suda,T., Takahashi,N. and Martin,T.J. (1992) Modulation of osteoclast differentiation. *Endocr. Rev.*, **13**, 66–80.

Taher,T.E., Tjin,E.P., Beuling,E.A., Borst,J., Spaargaren,M. and Pals,S.T. (2002) c-Cbl is involved in Met signaling in B cells and

mediates hepatocyte growth factor-induced receptor ubiquitination. *J. Immunol.*, **169**, 3793–3800.
Takahashi,N., Akatsu,T., Udagawa,N., Sasaki,T., Yamaguchi,A., Moseley,J.M., Martin,T.J. and Suda,T. (1988) Osteoblastic cells are involved in osteoclast formation. *Endocrinology*, **123**, 2600–2602.
Tanaka,S., Amling,M., Neff,L., Peyman,A., Uhlmann,E., Levy,J.B. and Baron,R. (1996) c-Cbl is downstream of c-Src in a signalling pathway necessary for bone resorption. *Nature*, **383**, 528–531.
Tanaka,S., Takahashi,T., Takayanagi,H., Miyazaki,T., Oda,H., Nakamura,K., Hirai,H. and Kurokawa,T. (1998) Modulation of osteoclast function by adenovirus vector-induced epidermal growth factor receptor. *J. Bone Miner. Res.*, **13**, 1714–1720.
Tanaka,S., Nakamura,I., Inoue,J., Oda,H. and Nakamura,K. (2003) Signal transduction pathways regulating osteoclast differentiation and function. *J. Bone Miner. Metab.*, **21**, 123–133.
Thompson,C.B. (1995) Apoptosis in the pathogenesis and treatment of disease. *Science*, **267**, 1456–1462.
Villunger,A., Scott,C., Bouillet,P. and Strasser,A. (2003) Essential role for the BH3-only protein Bim but redundant roles for Bax, Bcl-2 and Bcl-w in the control of granulocyte survival. *Blood*, **101**, 2393–2400.
Weston,C.R., Balmanno,K., Chalmers,C., Hadfield,K., Molton,S.A., Ley,R., Wagner,E.F. and Cook,S.J. (2003) Activation of ERK1/2 by ΔRaf-1: ER* represses Bim expression independently of the JNK or PI3K pathways. *Oncogene*, **22**, 1281–1293.
Whitfield,J., Neame,S.J., Paquet,L., Bernard,O. and Ham,J. (2001) Dominant-negative c-Jun promotes neuronal survival by reducing BIM expression and inhibiting mitochondrial cytochrome c release. *Neuron*, **29**, 629–643.
Wong,B.R., Besser,D., Kim,N., Arron,J.R., Vologodskaia,M., Hanafusa,H. and Choi,Y. (1999) TRANCE, a TNF family member, activates Akt/PKB through a signaling complex involving TRAF6 and c-Src. *Mol. Cell*, **4**, 1041–1049.
Yamaguchi,T., Okada,T., Takeuchi,K., Tonda,T., Ohtaki,M., Shinoda,S., Masuzawa,T., Ozawa,K. and Inaba,T. (2003) Enhancement of thymidine kinase-mediated killing of malignant glioma by BimS, a BH3-only cell death activator. *Gene Ther.*, **10**, 375–385.
Yang,Y., Fang,S., Jensen,J.P., Weissman,A.M. and Ashwell,J.D. (2000) Ubiquitin protein ligase activity of IAPs and their degradation in proteasomes in response to apoptotic stimuli. *Science*, **288**, 874–877.
Zong,W.X., Lindsten,T., Ross,A.J., MacGregor,G.R. and Thompson, C.B. (2001) BH3-only proteins that bind pro-survival Bcl-2 family members fail to induce apoptosis in the absence of Bax and Bak. *Genes Dev.*, **15**, 1481–1486.

Received July 10, 2003; revised October 27, 2003; accepted October 30, 2003

ARTHRITIS & RHEUMATISM
Vol. 48, No. 9, September 2003, pp 2682–2692
DOI 10.1002/art.11214

Suppression of Arthritic Bone Destruction by Adenovirus-Mediated Dominant-Negative Ras Gene Transfer to Synoviocytes and Osteoclasts

Aiichiro Yamamoto,[1] Akira Fukuda,[1] Hiroaki Seto,[1] Tsuyoshi Miyazaki,[1] Yuho Kadono,[1] Yasuhiro Sawada,[1] Ichiro Nakamura,[1] Hideki Katagiri,[2] Tomoichiro Asano,[2] Yoshiya Tanaka,[2] Hiromi Oda,[1] Kozo Nakamura,[1] and Sakae Tanaka[1]

Objective. **To determine the role of Ras-mediated signaling pathways in synovial cell activation and bone destruction in arthritic joints.**

Methods. **The E11 rheumatoid synovial cell line and primary synovial fibroblast-like cells (SFCs) from patients with rheumatoid arthritis (RA) were gene-transferred by replication-deficient adenovirus vector carrying the dominant-negative mutant of the ras gene (AxRasDN). The effects of RasDN overexpression on cellular proliferation, interleukin-1 (IL-1)–induced activation of mitogen-activated protein kinases (extracellular signal–regulated kinase [ERK], p38, c-Jun N-terminal kinase [JNK]), and IL-6 production by synovial cells were analyzed. The in vivo effects of Ras inhibition on synovial cell activation and arthritic bone destruction were analyzed by injection of AxRasDN into ankle joints of rats with adjuvant arthritis.**

Results. **AxRasDN markedly reduced the proliferation of RA SFCs. IL-1, a proinflammatory cytokine involved in RA pathology, induced activation of ERK, p38, and JNK in the cells. Adenovirus vector–mediated RasDN overexpression suppressed ERK activation, but not p38 or JNK activation, in SFCs. IL-6 is also an important proinflammatory cytokine, and RasDN inhibited IL-1–induced production of IL-6 by RA SFCs at both the transcriptional and protein levels. Injection of AxRasDN into ankle joints of rats with adjuvant arthritis ameliorated inflammation and suppressed bone destruction in the affected joints.**

Conclusion. **Ras-mediated signaling pathways are involved in the activation of RA SFCs and the destruction of bone in arthritic joints, suggesting that inhibition of Ras signaling can be a novel approach for RA treatment that targets both synovial cell activation and bone destruction in the RA joint.**

Dr. Tanaka's work was supported by a grant-in-aid from the Ministry of Education, Culture, Sports, Science, and Technology of Japan, and by health science research grants from the Ministry of Health and Welfare and Uehara Memorial Foundation. Dr. Oda's work was supported by a grant-in-aid from the Ministry of Education, Culture, Sports, Science, and Technology of Japan, and by a grant from the Japan Orthopaedic and Traumatology Foundation (no. 0113). Dr. Nakamura's work was supported by the Takeda Memorial Foundation.

[1]Aiichiro Yamamoto, MD, Akira Fukuda, MD, Hiroaki Seto, MD, Tsuyoshi Miyazaki, MD, Yuho Kadono, MD, Yasuhiro Sawada, MD, Ichiro Nakamura, MD, Hiromi Oda, MD, Kozo Nakamura, MD, Sakae Tanaka, MD, PhD: University of Tokyo, Tokyo, Japan; [2]Hideki Katagiri, MD, Tomoichiro Asano, MD, Yoshiya Tanaka, MD: University of Occupational and Environmental Health, School of Medicine, Kitakyushu, Japan.

Address correspondence and reprint requests to Sakae Tanaka, MD, PhD, Department of Orthopaedic Surgery, Faculty of Medicine, The University of Tokyo, 7-3-1 Hongo, Bunkyo-ku, Tokyo 113-0033, Japan. E-mail: TANAKAS-ORT@h.u-tokyo.ac.jp.

Submitted for publication December 9, 2002; accepted in revised form May 1, 2003.

Rheumatoid arthritis (RA) is a chronic, systemic inflammatory disease of unknown etiology that is characterized by invasive synovial hyperplasia, leading to progressive joint destruction. Rheumatoid synovial cells are not only morphologically characterized by their transformed appearance (1), but are also phenotypically transformed to proliferate abnormally (2,3). These cells invade bone and cartilage by producing an elevated amount of proinflammatory cytokines (4) and metalloproteinases (5) and by inducing differentiation and activation of osteoclasts (6,7), which are multinucleated cells exclusively responsible for bone resorption. We previously reported that synovial fibroblast-like cells (SFCs) obtained from the inflamed joints of RA patients can support osteoclast differenti-

ation from monocyte/macrophage lineage precursors in the presence of osteotropic factors such as 1,25-dihydroxyvitamin D_3 (8).

Small GTPase Ras, the protein product of protooncogene ras, is ubiquitously found in eukaryotic organisms. Ras is known to function as a downstream effector of cell-surface receptor tyrosine kinases (RTKs) and leads to activation of mitogen-activated protein kinase (MAPK) pathways, which in turn regulates the activities of nuclear transcription factors and gene transcriptions (9,10). In human cancer cells, oncogenic mutations of the Ras protein are frequently observed and contribute to the malignant growth properties of the cells. Although increased expression and mutations of Ras in RA synovial tissue have been reported (11–13), the function of Ras in RA pathology remains to be clarified.

In the present study, we utilized a replication-deficient adenovirus vector carrying the dominant-negative mutant of the ras gene (AxRasDN) to investigate the role of Ras in RA SFCs and osteoclasts in vitro and in vivo. Adenovirus-mediated overexpression of RasDN dramatically decreased the proliferation rate of RA SFCs and inhibited interleukin-1 (IL-1)–induced extracellular signal–regulated kinase (ERK) activation and IL-6 production in RA SFCs. Importantly, injection of RasDN virus into ankle joints of rats with adjuvant arthritis not only ameliorated the inflammatory reactions, but also suppressed bone destruction in arthritic joints.

MATERIALS AND METHODS

Animals and chemicals. Inbred male Lewis rats (6–7 weeks old) were purchased from Sankyo Laboratory Services (Tokyo, Japan). Dulbecco's minimum essential medium (DMEM) was purchased from Gibco BRL (Life Technologies, Rockville, MD), and fetal bovine serum (FBS) was from Sigma (St. Louis, MO). Antibodies against phospho-ERK, c-Jun N-terminal kinases (JNKs) (p46 and p54), phospho-JNKs (Thr183/Tyl185), p38 MAPK, and phospho-p38 MAPK (Thr180/Tyr182) were purchased from New England Biolabs (Beverly, MA). Anti-Ras and anti-ERK antibodies were purchased from Transduction Laboratories (Lexington, KY). Human recombinant IL-1β was purchased from Wako Pure Chemicals (Tokyo, Japan). Other chemicals and reagents used in this study were of analytic grade.

Synovial cell cultures. With the use of enzymatic digestion methods previously described (6,14), primary RA SFCs were obtained from the synovial tissues of 3 female patients (age range 50–65 years) who fulfilled the American College of Rheumatology (formerly, the American Rheumatism Association) criteria for RA (15). Written informed consent was given by each patient. The cells were suspended in DMEM containing 10% FBS and used for experiments after 3–6 passages. We also established the E11 synovial fibroblast cell line from SFCs of RA patients, as previously reported (16).

Adenovirus vector construction and gene transduction in vitro. The recombinant adenovirus vector carrying the β-galactosidase gene (AxLacZ) was kindly provided by Izumu Saito (University of Tokyo). The recombinant adenovirus vector carrying the dominant-negative ras gene (AxRasDN) (Ser-17 to Asn), under the control of CAG-cytomegalovirus immediate early enhancer, chicken β-actin promoter, and rabbit β-globin poly(A) signal promoter, was constructed by homologous recombination between the expression cosmid cassette and the parental virus genome in 293 cells, as described previously (17,18). The RasS17N mutant is a distinct class of Ras mutant that is membrane localized but GDP bound. Therefore, RasS17N fails to bind effector proteins, but instead binds tightly to guanine nucleotide exchange factors, sequestering them in nonproductive complexes and thereby preventing them from activating Ras. Titers of the viral stock were determined by the modified end-point cytopathic effect assay (19). The efficiency of infection is affected not only by the concentration of viruses and cells, but also by the ratio of viruses to cells, known as the multiplicity of infection (MOI). Infection of synovial cells by adenovirus vectors was carried out as described previously (20).

Western blotting. Cells were washed with ice-cold phosphate buffered saline, and then lysed by adding TNE buffer (1% Nonidet P40, 10 m*M* Tris HCl, pH 7.8, 150 m*M* NaCl, 1 m*M* EDTA, 2 m*M* Na_3VO_4, 10 m*M* NaF, and 10 mg/ml aprotinin). The lysates were clarified by centrifugation at 15,000 revolutions per minute for 20 minutes. An equal amount of protein was subjected to 10% sodium dodecyl sulfate (SDS)–polyacrylamide gel electrophoresis, transferred electrophoretically onto a nitrocellulose membrane, and probed sequentially with an appropriate primary antibody followed by a secondary antibody coupled with horseradish peroxidase (Promega, Madison, WI). Immunoreactive proteins were visualized by enhanced chemiluminescence Western blotting detection reagents (Amersham International, Arlington Heights, IL) following the procedure recommended by the supplier. The blots were stripped by incubating for 20 minutes in stripping buffer (2% SDS, 100 m*M* 2-mercaptoethanol, 62.5 m*M* Tris HCl, pH 6.7) at 50°C and reprobed with other antibodies.

Cell proliferation assay. E11 cells and primary SFCs were infected with AxLacZ or AxRasDN at the indicated MOI. Forty-eight hours after infection, 4×10^4 cells were plated on culture plates (day 0). On days 1, 2, and 3, the cells were recovered by trypsin-EDTA treatment, and their number was counted. On day 0, cellular proliferation was also determined using a cell proliferation assay kit (Amersham International) involving immunostaining for 5-bromo-2'-deoxyuridine (BrdU), a thymidine analog, incorporated into replicating DNA according to the manufacturer's protocol.

Northern blot analysis. E11 cells were infected with either AxLacZ or AxRasDN at 100 MOI. After 48 hours of inoculation, the cells were treated with 25 ng/ml IL-1β for varying times, and total RNA was extracted using acid guani-

dinium isothiocyanate–phenol–chloroform (Isogen; Nippon Gene, Toyama, Japan) according to the manufacturer's protocol. Equal amounts (15 mg) of RNA were denatured in formaldehyde, separated on 1% agarose gel, and transferred to a nitrocellulose membrane (Hybond-N; Amersham Pharmacia Biotech, Little Chalfont, UK) followed by ultraviolet crosslinking. The blots were hybridized with a complementary DNA probe labeled with α-^{32}P-dCTP (NEM Life Science Products, Boston, MA) and Ready-To-Go DNA Labeling Beads (Amersham Pharmacia Biotech). The human IL-6 probe was the polymerase chain reaction product of synoviocytes, and detection was carried out using the primers described previously (21). The expression level of IL-6 was quantified by scanning the blots by densitometry (Luminous Imager; Aisin Cosmos, Aichi, Japan).

Enzyme-linked immunosorbent assay (ELISA) for IL-6. Primary SFCs were infected with either AxLacZ or AxRasDN at 100 MOI. Twenty-four hours after infection, the cells were recovered by trypsin-EDTA treatment and replated on 96-well microtiter plates (10^5/well). The cells were cultured in serum-free medium for a further 24 hours and treated with or without 100 ng/ml IL-1β. The conditioned medium was recovered and the IL-6 concentration in the medium was determined using a human IL-6 ELISA kit (Fujirei Bio, Tokyo, Japan).

Induction of adjuvant arthritis. Inbred, 6–7-week-old male Lewis rats were immunized by subcutaneous injection into the base of the tail (day 0) with 100 ml liquid paraffin containing 0.6 mg/ml *Mycobacterium butyricum* (Difco, Detroit, MI). Arthritis of the bilateral ankle joints developed in 100% of the animals after day 7.

Therapeutic protocol. For introduction of viruses into the rat ankle joints, the right ankles of 20 rats were immunized as described above (day 0). On days 7 and 14, the rats of the LacZ group and the RasDN group (each n = 10) were injected with 30 ml of AxLacZ or AxRasDN (3.0×10^8 virus particles per rat) into the inflamed right ankle joint space. Therapeutic effects of the injected viruses were examined by determining arthritis scores (scale of 0–4, with 4 being the most severe) and measuring paw volume on days 7, 14, 21, 28, 35, and 42, with the rats placed under inhalation anesthesia with diethyl ether. For radiologic and histologic examinations, the rats were killed on day 42.

All of these evaluations were performed by a single observer who was blinded to the treatment group. The arthritis score, paw volume, and radiologic score were determined as previously described (22,23). Histologic evaluation of the joint destruction was performed as previously described (24). Serial sections were stained for tartrate-resistant acid phosphatase (TRAP) (25), and TRAP-positive multinucleated osteoclast-like cells (OCLs) on bone surfaces of the talotibial, talocalcaneal, and calcaneonavicular joints were quantified microscopically. Three microscopic fields were randomly selected in each joint and the number of TRAP-positive OCLs was counted. A mean number of 9 fields/3 joints was calculated for each section.

Statistical analysis. All values are expressed as the mean ± SD. Data were statistically analyzed by analysis of variance.

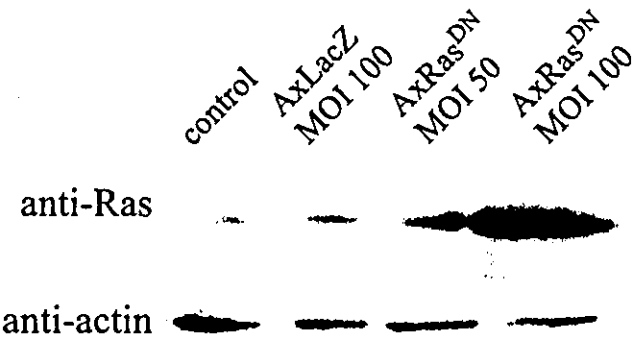

Figure 1. Adenovirus vector–mediated overexpression of the dominant-negative mutant of the ras gene (RasDN) in rheumatoid arthritis synovial cells. E11 cells were infected with either the recombinant adenovirus vector carrying the β-galactosidase gene (AxLacZ) or that for RasDN (AxRas^{DN}) at the indicated multiplicities of infection (MOI). Forty-eight hours after infection, the expression of RasDN was examined by Western blotting with an antibody specific for Ras. AxRas^{DN} induced the expression of RasDN in the cells in an MOI-dependent manner. The blots were stripped and reprobed with an antibody for β-actin (anti-actin) to show that an equal amount of protein was loaded. The molecular weights of Ras and β-actin were 21 kd and 43 kd, respectively.

RESULTS

Inhibition of cell growth by adenovirus-mediated RasDN overexpression. Previous studies demonstrated that the adenovirus vector can efficiently transduce genes into RA SFCs in vitro (25). To analyze the effect of RasDN overexpression, RA SFCs were infected with either AxLacZ or AxRasDN. First, to determine the efficiency of the vector, the expression of RasDN was examined by Western blotting with an antibody specific for Ras. As shown in Figure 1, Western blot analysis revealed that AxRasDN induced the expression of RasDN in E11 cells in an MOI-dependent manner.

The effect of adenovirus-mediated RasDN overexpression on cell proliferation was evaluated by cell count and BrdU incorporation into DNA of replicating cells. AxRasDN remarkably reduced the proliferation rate of E11 cells and primary SFCs in an MOI-dependent manner, as compared with the effects of AxLacZ, which induced an increase in cell number (Figure 2A). The ratio of proliferating (BrdU-positive) cells was also reduced by AxRasDN (Figure 2B).

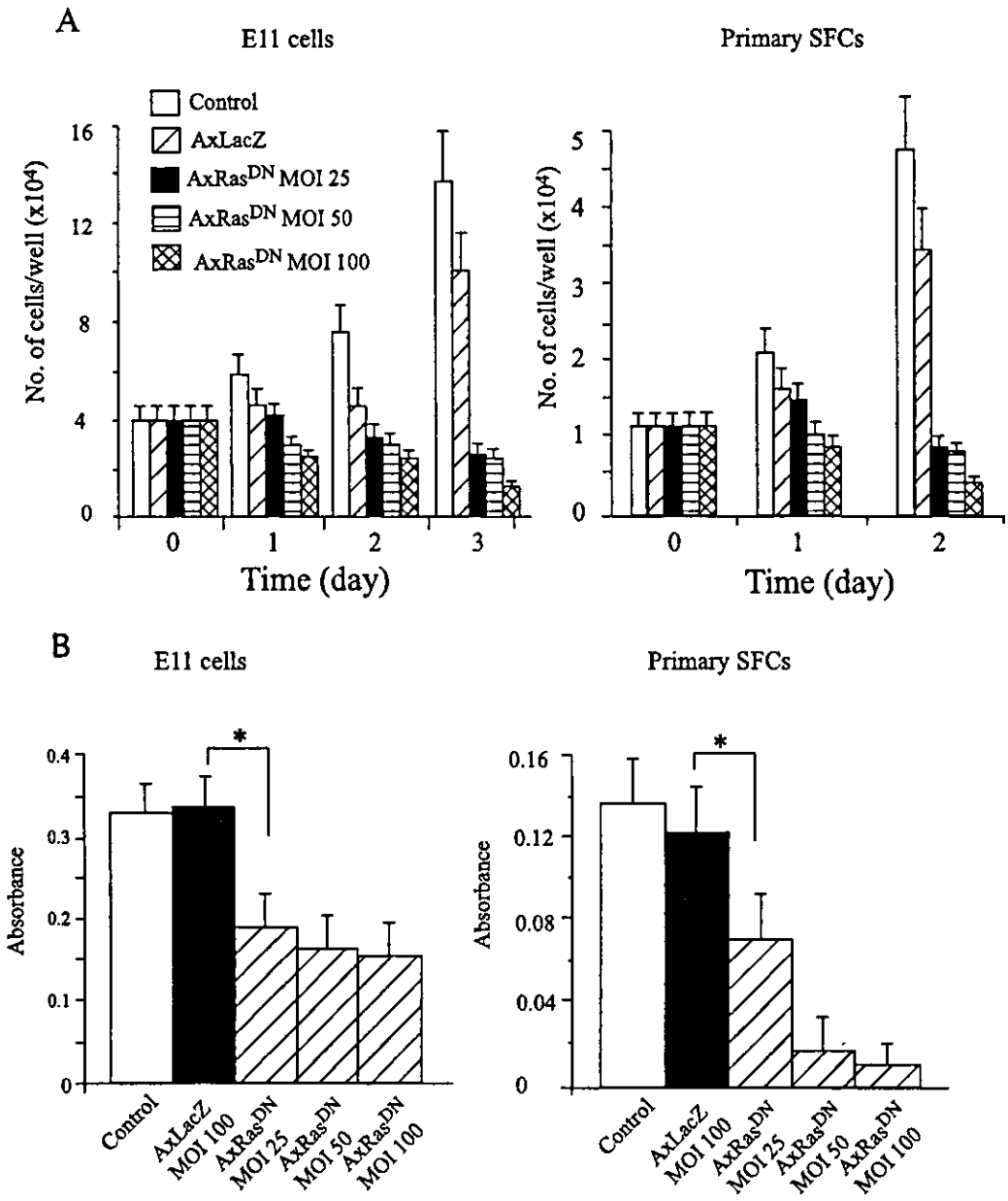

Figure 2. RasDN-mediated inhibition of rheumatoid synovial cell proliferation. E11 cells and primary synovial fibroblast-like cells (SFCs) were infected with either AxLacZ or $AxRas^{DN}$ at the indicated MOI. Forty-eight hours after infection, 4×10^4 cells were plated on culture plates (day 0). **A,** Cell counts on days 1, 2, and 3. Cellular proliferation was inhibited by RasDN overexpression in an MOI-dependent manner, in E11 cells and primary SFCs. **B,** Cell proliferation determined by quantification of 5-bromo-2′-deoxyuridine incorporated into replicating DNA. Cell proliferation was inhibited by RasDN overexpression in an MOI-dependent manner, in E11 cells and primary SFCs. * = $P < 0.01$ versus LacZ virus–infected cells. See Figure 1 for other definitions.

Prevention of IL-1–induced MAPK activation in RA SFCs by adenovirus-mediated RasDN overexpression. IL-1 is a potent proinflammatory cytokine that increases the expression of a wide variety of genes important for immunity and inflammation in target cells, and plays a central role in inflammatory responses and RA pathology (4,26). IL-1 is known to activate 4 protein kinase cascades in cells, i.e., the transcription factor

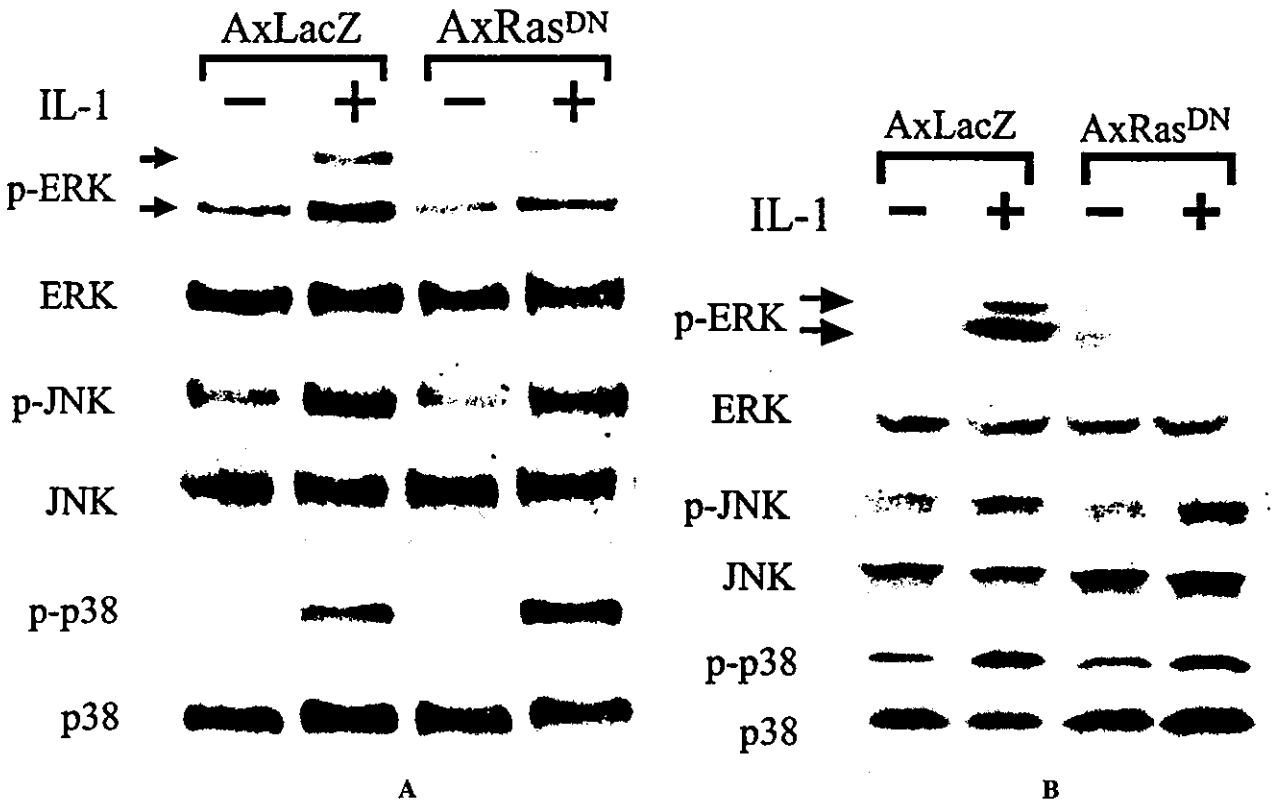

Figure 3. Prevention of interleukin-1β (IL-1)–induced mitogen-activated protein kinase (MAPK) activation by RasDN overexpression. Primary RA synovial fibroblast-like cells (SFCs) (**A**) and E11 cells (**B**) were infected with either AxLacZ or $AxRas^{DN}$ at 100 MOI. Twenty-four hours after infection, the culture medium was changed to serum-free medium, and after another 24 hours of incubation, the cells were treated with 25 ng/ml IL-1β for varying times and lysed. An equal amount of protein was subjected to 10% sodium dodecyl sulfate–polyacrylamide gel electrophoresis, transferred onto a nitrocellulose membrane, and probed sequentially with antibodies against the active forms of extracellular signal–regulated kinase (ERK), c-Jun N-terminal kinase (JNK), and p38 (phospho-ERK [p-ERK], p-JNK, and p-p38, respectively). The blots were stripped and reprobed with the antibody specific for the inactive form of each MAPK to show that an equal amount of protein was applied. Rapid induction of activation of all 3 MAPKs was seen in AxLacZ-infected cells. RasDN overexpression prevented ERK activation, but not JNK or p38 activation, in both primary SFCs (**A**) and E11 cells (**B**). See Figure 1 for other definitions.

nuclear factor κB (NF-κB) (26) and MAPK cascades, including the stress-activated kinases p38 MAPK and JNK and the classic kinase ERK (27–29). Primary RA SFCs and E11 cells were infected with either AxLacZ or AxRasDN at 100 MOI, and 48 hours after infection, the cells were stimulated with 25 ng/ml IL-1β. As shown in Figure 3, IL-1 rapidly induced activation of ERK, JNK, and p38 in these cells. IL-1–induced ERK activation was remarkably prevented by overexpression of RasDN, whereas it had little effect on JNK or p38 activation in both primary RA SFCs and E11 cells (Figures 3A and B, respectively). This observation reveals the essential role of Ras in IL-1–induced ERK activation in RA SFCs. The experiments were performed using SFCs derived from 3 different patients, each of which produced similar results.

Reduction of IL-6 production from RA SFCs at the messenger RNA (mRNA) and protein level by adenovirus-mediated RasDN overexpression. IL-6 has a variety of biologic activities, including activation of B and T cells, stimulation of fever, and release of acute-phase response proteins (30,31). Guerne et al previously reported the spontaneous production of an elevated amount of IL-6 and a potent induction of IL-6 synthesis by IL-1 in RA synovial cells (32). The IL-6 cytokine is involved in the proliferation of RA synovial cells in cooperation with the soluble IL-6 receptor and may play an important role in RA pathogenesis (33). To deter-

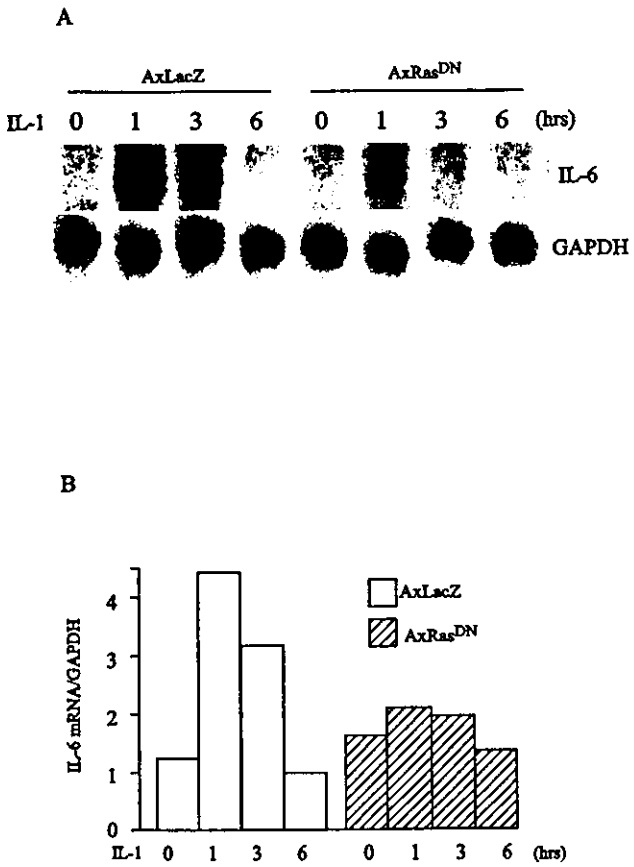

Figure 4. Inhibition of interleukin-1β (IL-1)–induced transcription of IL-6 mRNA in RA synoviocytes by RasDN overexpression. **A**, In AxLacZ-infected cells, IL-6 mRNA transcription was induced from 1 hour to 3 hours after treatment with IL-1β. In AxRasDN-infected cells, the process was clearly inhibited. **B**, Induction of IL-6 mRNA transcription is shown normalized to the blot of GAPDH, for both the AxLacZ and AxRas^{DN} groups. See Figure 1 for other definitions.

mine the effect of RasDN overexpression on IL-1–induced IL-6 synthesis in RA SFCs, E11 cells and primary SFCs were infected with either AxLacZ or AxRasDN at 100 MOI. Forty-eight hours after inoculation, the cells were further incubated with or without 25 ng/ml IL-1β. The IL-6 mRNA level in the cells was detected by Northern blot analysis, and the IL-6 concentration in conditioned medium was measured by ELISA. Northern blotting showed a dramatic decrease in IL-1–induced transcription of IL-6 mRNA in AxRasDN-infected cells (Figures 4A and B). ELISA for IL-6 showed that overexpression of RasDN markedly reduced the basal production of IL-6 as well as the IL-1–induced production of IL-6 in RA SFCs (Figures 5A and B, respectively).

Amelioration of inflammation and suppression of bone destruction by AxRasDN in arthritic joints of rats with adjuvant arthritis. To analyze the in vivo effect of overexpression of RasDN on synovial cell activation and arthritic bone destruction, either AxLacZ or AxRasDN was injected into the inflamed ankle joints of rats with adjuvant arthritis, and the severity of the disease was evaluated by arthritis score, paw volume, and radiologic and pathohistologic examinations. On days 35–42, the arthritis scores of the AxRasDN-injected rats were significantly improved compared with those of the AxLacZ-injected animals (Figure 6A). The increase in paw volume was also significantly decreased by AxRasDN injection as compared with that in the AxLacZ group (Figure 6B). When the rats were killed on day 42, the ankle joints of AxLacZ-injected rats showed radiologic findings of severe joint destruction, which was characterized by joint space narrowing, erosion, and periarticular osteoporosis (Figure 6C), but these destructive changes were remarkably suppressed in the AxRasDN-injected rats (Figure 6D). These significant differences were further confirmed by radiologic scoring (Figure 6E).

The pathohistologic examinations revealed that AxRasDN injection suppressed synovial hyperplasia and caused a marked reduction in pannus formation and decrease in the infiltration of inflammatory cells

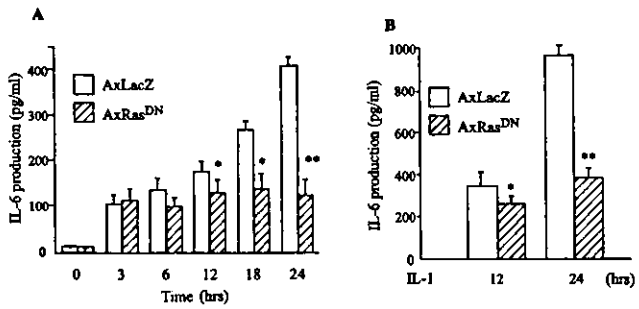

Figure 5. Inhibition of interleukin-6 (IL-6) production in primary RA synovial fibroblast-like cells (SFCs) by RasDN overexpression. **A**, Overexpression of RasDN markedly reduced the basal production of IL-6 by RA primary SFCs. **B**, IL-1β–induced production of IL-6 was also reduced in AxRasDN-infected cells. Bars show the mean and SD from 5 independent experiments, using RA SFCs derived from 1 patient. * = $P < 0.01$ and ** = $P < 0.001$, versus AxLacZ-infected cells. See Figure 1 for other definitions.

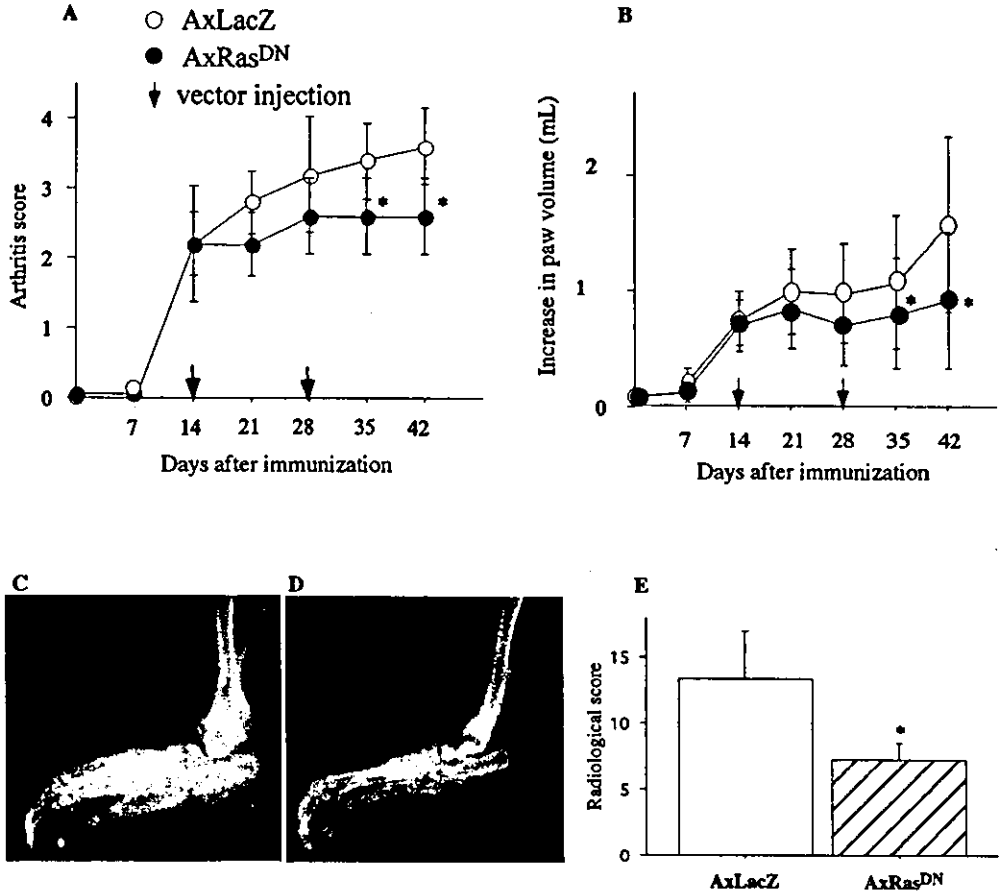

Figure 6. Therapeutic effects of $AxRas^{DN}$ injection on rat adjuvant arthritis. All rats were immunized with a subcutaneous injection of adjuvant in the base of the tail (day 0). Viruses were then intraarticularly injected into the right ankles on days 7 and 14. Bars show the mean ± SD of 10 rats per group. A, Effects of $AxRas^{DN}$ injection, evaluated by arthritis score. The arthritis score of the $AxRas^{DN}$ group was significantly lower than that of the AxLacZ group on days 35 and 42. B, Effects of $AxRas^{DN}$ injection, evaluated by the increase in paw volume. The increase in paw volume of the $AxRas^{DN}$ group was significantly less than that of the AxLacZ group on days 35 and 42. C, The radiologic findings in the right ankles of AxLacZ-injected rats indicate severe joint destruction. D, The radiologic findings in the right ankles of $AxRas^{DN}$-injected rats show minimal destructive changes in the joint. E, The radiologic score of the $AxRas^{DN}$-injected ankles was significantly decreased in comparison with that of the AxLacZ group. * = $P < 0.01$ versus AxLacZ-injected joints. See Figure 1 for definitions.

(AxLacZ versus AxRasDN group in Figures 7A and B, respectively), which was confirmed by pathohistologic scoring (Figure 7C). The number of osteoclasts positively staining for TRAP was remarkably reduced in the AxRasDN-injected group compared with that in the AxLacZ group (Figure 7E versus Figure 7D, respectively, and Figure 7F).

DISCUSSION

Ras is encoded by 3 ras protooncogenes, H-, K-, and N-Ras, and belongs to a superfamily of GTPases. The encoded, highly homologous Ras proteins are positioned at the inner surface of the plasma membrane and play a crucial role in transmitting growth factor signals to the cell nucleus (34). Similar to other GTPases, Ras proteins function as switches cycling between 2 distinct conformational states: active in GTP-bound form and inactive in GDP-bound form (9). Oncogenic mutations lock Ras into its active state, up-regulate cell growth, and induce cell transformation.

Activating mutations of the ras protooncogene occur in ~30% of all human tumors (35), primarily in

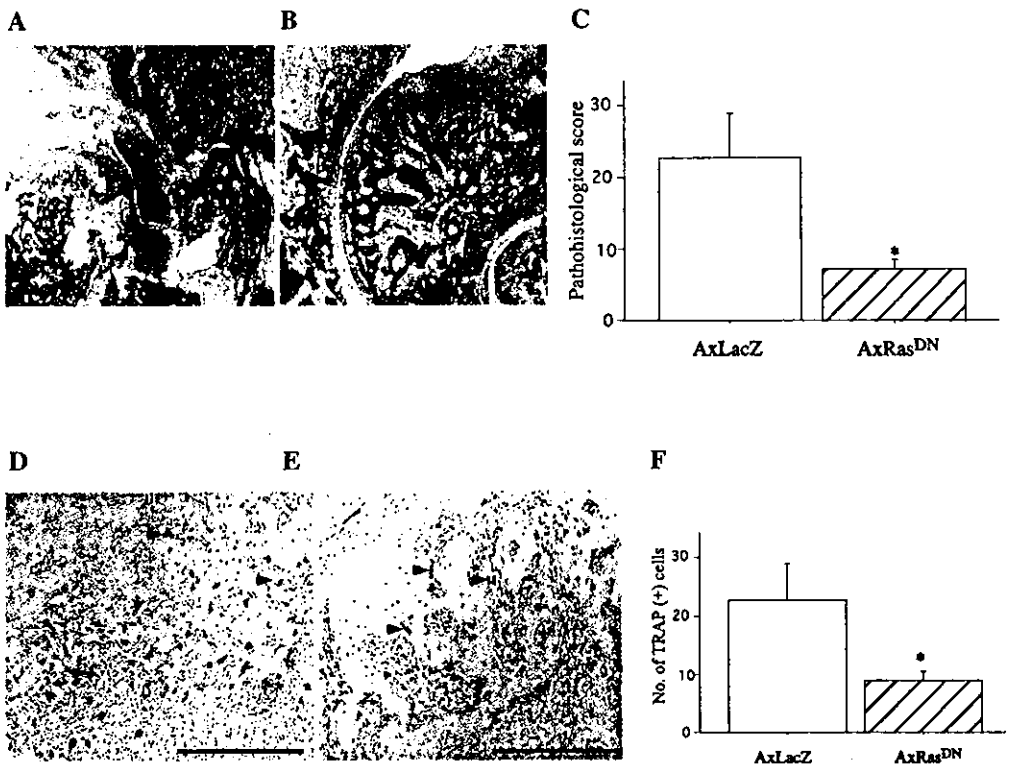

Figure 7. Pathohistologic evaluation of the joint destruction in serial sections of rat arthritic ankles. **A,** Pathohistologic findings in a representative AxLacZ-injected ankle indicate synovial hyperplasia and destructive change in the articular cartilage and bone. **B,** Pathohistologic findings in a representative $AxRas^{DN}$-injected right ankle show synovial hyperplasia with invasion into subchondral bone and marked suppression of the destruction of bone and cartilage. In **A** and **B,** the **open arrowhead** and **solid arrowhead** indicate the talotibial and talocalcaneal joint, respectively. **C,** The pathologic score of the $AxRas^{DN}$-injected ankles was significantly decreased in comparison with that of the AxLacZ group. **D** and **E,** Tartrate-resistant acid phosphatase (TRAP)–positive multinucleated osteoclast-like cells (OCLs) on bone surfaces of the talotibial, talocalcaneal, and calcaneonavicular joints were quantified microscopically. Three microscopic fields were randomly selected in each joint and the number of TRAP-positive OCLs was counted. A mean number of 9 fields/3 joints was calculated for each section. In a TRAP-stained section of an AxLacZ-injected ankle **(D)** and an $AxRas^{DN}$-injected ankle **(E),** the **arrowheads** indicate TRAP-positive multinucleated OCLs. Bar = 500 mm. **F,** Quantification of TRAP-positive multinucleated OCLs on bone surfaces. The number of TRAP-positive OCLs was significantly decreased in the $AxRas^{DN}$ group. * = $P < 0.001$ versus AxLacZ-injected joints. See Figure 1 for other definitions.

pancreatic (90%), sporadic colorectal (50%), and lung (40%) carcinomas and myeloid leukemia (30%). Because Ras is a key regulator of mitogenic signals, aberrant function of upstream elements such as RTKs can also result in Ras activation in the absence of mutations in Ras itself (36). In fact, overexpression of RTKs such as HER2/Neu/ErbB2 or the epidermal growth factor receptor (EGFR) is frequently observed in breast cancer (25–30%) (37), and overexpression of platelet-derived growth factor receptor or of wild-type or truncated EGFR is prevalent in gliomas and glioblastomas (40–50%), which are tumor types in which Ras mutations are rare (38–41). In RA and animal models of arthritis, transformed-appearing synovial cells with large, pale nuclei, prominent nucleoli, and abundant cytoplasm are found adjacent to the affected cartilage and bone of the joint (42), and these cells in culture have a tendency to grow in disorganized monolayers, proliferate in an anchorage-independent manner, lack contact inhibition, and form microfoci (43–46). Although expression of Ras and its oncogenic mutations has been reported in RA synovial cells (13,47,48), the precise role of Ras in RA pathology remains to be clarified.

In the present study, we analyzed the role of Ras

in synovial cell function and joint destruction in arthritic rats using the adenovirus vector encoding the dominant-negative mutant of ras (AxRasDN), and demonstrated that the overexpression of RasDN protein in cultured RA SFCs strongly suppressed their proliferation rate. The RA synovial environment is replete with proinflammatory cytokines, which have been described as exerting a synergistic mitogenic effect on synovial cells, resulting in altered rates of proliferation (49). Ras is a central mediator of such growth factor–induced cell proliferation, is required throughout the G1 phase, and is essential for S-phase progression of fibroblasts (50). Therefore, the inhibitory effect of RasDN overexpression on RA SFC proliferation may be explained by modulation of the cell cycle activated by these mitogenic stimuli.

The MAPKs are a family of kinases that respond to diverse stimuli and are composed of parallel protein kinase cascades. There are 3 well-defined pathways: ERK1 and ERK2 (also referred to as p42/p44 MAPKs), JNKs, and the p38 MAPKs (51). Activation of certain cytokine receptors, growth factor RTKs, and G protein–coupled receptors activates the ERKs. The p38 protein kinases are induced by lipopolysaccharide, proinflammatory cytokines, and cellular stresses such as osmotic shock. The JNKs are activated by a variety of stimuli, including ultraviolet irradiation, protein-synthesis inhibitors, and cytokines. The MAPK families regulate a number of transcription factors, with subsequent activation of cytokine gene expression and matrix metalloproteinases (52). Constitutive activation of ERK, JNK, and p38 MAPK is found almost exclusively in synovial tissues from RA patients, but is not found in osteoarthritis patients (53).

IL-1 is considered to be a major activator of MAPK pathways in cultured human synovial cells, and plays critical roles in the joint pathology of RA (53). The introduction of RasDN in RA SFCs suppressed IL-1–induced ERK activation, but not JNK or p38 activation, as shown in Figure 3, indicating that ERK signals from IL-1 receptors utilize Ras in RA SFCs. We performed similar experiments using human epithelial carcinoma cell–derived HeLa cells, and obtained basically similar results. Therefore, the effect of RasDN overexpression on IL-1–induced ERK activation is not specific to RA SFCs. A potential convergence point of IL-1 and the Ras signaling pathway is tumor necrosis factor receptor–associated factor 6 (TRAF6), which is an adapter protein necessary for IL-1 signaling (54–56). Recently, McDermott and O'Neill reported that IL-1 induces activation of Ras, and its association with IL-1 receptor–associated kinase, TRAF6, and transforming growth factor β1–activated kinase is important for IL-1–induced p38 activation (57). Further investigations are needed to better characterize the mechanisms of signal cross-talk between IL-1 and Ras signaling pathways.

IL-6 is a proinflammatory cytokine whose synthesis is induced by a variety of stimuli, including IL-1, and has been suggested to be involved in the pathogenesis of RA. IL-6 is abundantly detected in the synovial fluid and the serum of RA patients, and correlates with the severity of the disease (58,59). RA SFCs produce a large amount of IL-6 (32), and IL-6 stimulates the proliferation of RA synovial cells and formation of osteoclasts in cooperation with the soluble IL-6 receptor (33,60). IL-6 gene transcription is constitutively activated in RA SFCs, owing to the activation of NF-κB and C-promoter binding factor 1 (61). Furthermore, antigen-induced arthritis is poorly developed in IL-6–deficient mice (62), and blockage of IL-6 receptors suppresses murine collagen-induced arthritis (63). These reports suggest the critical involvement of IL-6 in autoimmune arthritis. RasDN overexpression suppressed IL-1–induced expression of IL-6 mRNA in RA SFCs, and the basal and IL-1–induced secretion of IL-6 by RA SFCs were also significantly reduced, indicating that Ras signaling is also important in activated transcription of this cytokine by RA SFCs. The mechanism by which RasDN inhibits IL-6 expression remains elusive, but the possible mechanism could be RasDN-mediated suppression of p38 MAPK activation, which is necessary for IL-6 mRNA stabilization, as recently described (64).

These results suggest that Ras signaling plays a critical role in the proliferation and activation of RA SFCs. Moreover, we recently reported that adenovirus vector–mediated overexpression of RasDN induced rapid apoptosis of osteoclasts, which are primary cells responsible for bone destruction (65). Therefore, suppressing Ras signaling can be a potent therapeutic approach for ameliorating the bone and joint destruction of RA. Finally, we demonstrated that AxRasDN virus gene therapy ameliorated arthritic changes and bone destruction in rats with adjuvant arthritis. The severity of inflammatory reactions in the ankle joints of these rats, as assessed by arthritis score and paw volume, was significantly improved by the intraarticular injection of AxRasDN. The suppression of joint destruction was confirmed by radiologic and pathohistologic examinations. Taken together, our data indicate that these therapeutic effects of AxRasDN on the inflammatory reaction and bone destruction in arthritic rats resulted from direct inhibition of RA SFC proliferation and/or activation as well as from the suppression of osteoclast

activity, although further investigation will be required to identify the mechanism in detail.

In summary, intervention into intracellular signal transduction pathways of RA SFCs and osteoclasts by adenovirus-mediated gene transfer of dominant-negative Ras might lead to a novel therapeutic strategy for preventing the joint breakdown associated with RA. There will be no cure for RA until its etiology is elucidated, but our results may lead to the development of novel types of therapeutics for the treatment of RA, such as adenovirus vector–mediated gene therapy to target Ras and farnesyltransferase inhibitors to inhibit Ras pathways.

ACKNOWLEDGMENTS

The authors thank R. Yamaguchi and M. Ikeuchi (Department of Orthopaedic Surgery, University of Tokyo), who provided expert technical assistance.

REFERENCES

1. Fassbender HG. Histomorphological basis of articular cartilage destruction in rheumatoid arthritis. Coll Relat Res 1983;3:141–55.
2. Hamilton JA. Hypothesis: in vitro evidence for the invasive and tumor-like properties of the rheumatoid pannus. J Rheumatol 1983;10:845–51.
3. Yocum DE, Lafyatis R, Remmers EF, Schumacher HR, Wilder RL. Hyperplastic synoviocytes from rats with streptococcal cell wall-induced arthritis exhibit a transformed phenotype that is thymic-dependent and retinoid inhibitable. Am J Pathol 1988;132: 38–48.
4. Isomaki P, Punnonen J. Pro- and anti-inflammatory cytokines in rheumatoid arthritis. Ann Med 1997;29:499–507.
5. McCachren SS. Expression of metalloproteinases and metalloproteinase inhibitor in human arthritic synovium. Arthritis Rheum 1991;34:1085–93.
6. Takayanagi H, Oda H, Yamamoto S, Kawaguchi H, Tanaka S, Nishikawa T, et al. A new mechanism of bone destruction in rheumatoid arthritis: synovial fibroblasts induce osteoclastogenesis. Biochem Biophys Res Commun 1997;240:279–86.
7. Gravallese EM, Harada Y, Wang JT, Gorn AH, Thornhill TS, Goldring SR. Identification of cell types responsible for bone resorption in rheumatoid arthritis and juvenile rheumatoid arthritis. Am J Pathol 1998;152:943–51.
8. Takayanagi H, Iizuka H, Juji T, Nakagawa T, Yamamoto A, Miyazaki T, et al. Involvement of receptor activator of nuclear factor κB ligand/osteoclast differentiation factor in osteoclastogenesis from synoviocytes in rheumatoid arthritis. Arthritis Rheum 2000;43:259–69.
9. Bourne HR, Sanders DA, McCormick F. The GTPase superfamily: conserved structure and molecular mechanism. Nature 1991; 349:117–27.
10. Campbell SL, Khosravi-Far R, Rossman KL, Clark GJ, Der CJ. Increasing complexity of Ras signaling. Oncogene 1998;17: 1395–413.
11. Gay S, Gay RE. Cellular basis and oncogene expression of rheumatoid joint destruction. Rheumatol Int 1989;9:105–13.
12. Trabandt A, Aicher WK, Gay RE, Sukhatme VP, Nilson-Hamilton M, Hamilton RT, et al. Expression of the collagenolytic and Ras-induced cysteine proteinase cathepsin L and proliferation-associated oncogenes in synovial cells of MRL/I mice and patients with rheumatoid arthritis. Matrix 1990;10:349–61.
13. Roivainen A, Soderstrom KO, Pirila L, Aro H, Kortekangas P, Merilahti-Palo R, et al. Oncoprotein expression in human synovial tissue: an immunohistochemical study of different types of arthritis. Br J Rheumatol 1996;35:933–42.
14. Burmester GR, Dimitriu-Bona A, Waters SJ, Winchester RJ. Identification of three major synovial lining cell populations by monoclonal antibodies directed to Ia antigens and antigens associated with monocytes/macrophages and fibroblasts. Scand J Immunol 1983;17:69–82.
15. Arnett FC, Edworthy SM, Bloch DA, McShane DJ, Fries JF, Cooper NS, et al. The American Rheumatism Association 1987 revised criteria for the classification of rheumatoid arthritis. Arthritis Rheum 1988;31:315–24.
16. Abe M, Tanaka Y, Saito K, Shirakawa F, Koyama Y, Goto S, et al. Regulation of interleukin (IL)-1β gene transcription induced by IL-1β in rheumatoid synovial fibroblast-like cells, E11, transformed with simian virus 40 large T antigen. J Rheumatol 1997; 24:420–9.
17. He TC, Zhou S, da Costa LT, Yu J, Kinzler KW, Vogelstein B. A simplified system for generating recombinant adenoviruses. Proc Natl Acad Sci U S A 1998;95:2509–14.
18. Miyake S, Makimura M, Kanegae Y, Harada S, Sato Y, Takamori K, et al. Efficient generation of recombinant adenoviruses using adenovirus DNA-terminal protein complex and a cosmid bearing the full-length virus genome. Proc Natl Acad Sci U S A 1996;93: 1320–4.
19. Kanegae Y, Makimura M, Saito I. A simple and efficient method for purification of infectious recombinant adenovirus. Jpn J Med Sci Biol 1994;47:157–66.
20. Tanaka S, Takahashi T, Takayanagi H, Miyazaki T, Oda H, Nakamura K, et al. Modulation of osteoclast function by adenovirus vector-induced epidermal growth factor receptor. J Bone Miner Res 1998;13:1714–20.
21. Chandrasekar B, Melby PC, Troyer DA, Freeman GL. Induction of proinflammatory cytokine expression in experimental acute Chagasic cardiomyopathy. Biochem Biophys Res Commun 1996; 223:365–71.
22. Zhang H, Yang Y, Horton JL, Samoilova EB, Judge TA, Turka LA, et al. Amelioration of collagen-induced arthritis by CD95 (Apo-1/Fas)-ligand gene transfer. J Clin Invest 1997;100:1951–7.
23. Ackerman NR, Rooks WH II, Shott L, Genant H, Maloney P, West E. Effects of naproxen on connective tissue changes in the adjuvant arthritic rat. Arthritis Rheum 1979;22:1365–74.
24. Takayanagi H, Juji T, Miyazaki T, Iizuka H, Takahashi T, Isshiki M, et al. Suppression of arthritic bone destruction by adenovirus-mediated csk gene transfer to synoviocytes and osteoclasts. J Clin Invest 1999;104:137–46.
25. Takahashi N, Yamana H, Yoshiki S, Roodman GD, Mundy GR, Jones SJ, et al. Osteoclast-like cell formation and its regulation by osteotropic hormones in mouse bone marrow cultures. Endocrinology 1988;122:1373–82.
26. O'Neill LA, Greene C. Signal transduction pathways activated by the IL-1 receptor family: ancient signaling machinery in mammals, insects, and plants. J Leukoc Biol 1998;63:650–7.
27. Zhang S, Han J, Sells MA, Chernoff J, Knaus UG, Ulevitch RJ, et al. Rho family GTPases regulate p38 mitogen-activated protein kinase through the downstream mediator Pak1. J Biol Chem 1995;270:23934–6.
28. Raingeaud J, Gupta S, Rogers JS, Dickens M, Han J, Ulevitch RJ, et al. Pro-inflammatory cytokines and environmental stress cause p38 mitogen-activated protein kinase activation by dual phosphorylation on tyrosine and threonine. J Biol Chem 1995;270:7420–6.
29. Kyriakis JM, Banerjee P, Nikolakaki E, Dai T, Rubie EA, Ahmad MF, et al. The stress-activated protein kinase subfamily of c-Jun kinases. Nature 1994;369:156–60.

30. Kishimoto T, Akira S, Taga T. Interleukin-6 and its receptor: a paradigm for cytokines. Science 1992;258:593–7.
31. Kopf M, Baumann H, Freer G, Freudenberg M, Lamers M, Kishimoto T, et al. Impaired immune and acute-phase responses in interleukin-6-deficient mice. Nature 1994;368:339–42.
32. Guerne PA, Zuraw BL, Vaughan JH, Carson DA, Lotz M. Synovium as a source of interleukin 6 in vitro: contribution to local and systemic manifestations of arthritis. J Clin Invest 1989;83: 585–92.
33. Mihara M, Moriya Y, Kishimoto T, Ohsugi Y. Interleukin-6 (IL-6) induces the proliferation of synovial fibroblastic cells in the presence of soluble IL-6 receptor. Br J Rheumatol 1995;34:321–5.
34. Moodie SA, Willumsen BM, Weber MJ, Wolfman A. Complexes of Ras.GTP with Raf-1 and mitogen-activated protein kinase kinase. Science 1993;260:1658–61.
35. Bos JL. ras oncogenes in human cancer: a review. Cancer Res 1989;49:4682–9.
36. Lowe PN, Skinner RH. Regulation of Ras signal transduction in normal and transformed cells. Cell Signal 1994;6:109–23.
37. Slamon DJ, Clark GM, Wong SG, Levin WJ, Ullrich A, McGuire WL. Human breast cancer: correlation of relapse and survival with amplification of the HER-2/neu oncogene. Science 1987;235: 177–82.
38. Guha A, Dashner K, Black PM, Wagner JA, Stiles CD. Expression of PDGF and PDGF receptors in human astrocytoma operation specimens supports the existence of an autocrine loop. Int J Cancer 1995;60:168–73.
39. Ekstrand AJ, Sugawa N, James CD, Collins VP. Amplified and rearranged epidermal growth factor receptor genes in human glioblastomas reveal deletions of sequences encoding portions of the N- and/or C-terminal tails. Proc Natl Acad Sci U S A 1992;89:4309–13.
40. Libermann TA, Nusbaum HR, Razon N, Kris R, Lax I, Soreq H, et al. Amplification, enhanced expression and possible rearrangement of EGF receptor gene in primary human brain tumours of glial origin. Nature 1985;313:144–7.
41. Guha A, Feldkamp MM, Lau N, Boss G, Pawson A. Proliferation of human malignant astrocytomas is dependent on Ras activation. Oncogene 1997;15:2755–65.
42. Muller-Ladner U, Kriegsmann J, Gay RE, Gay S. Oncogenes in rheumatoid arthritis. Rheum Dis Clin North Am 1995;21:675–90.
43. Lafyatis R, Remmers EF, Roberts AB, Yocum DE, Sporn MB, Wilder RL. Anchorage-independent growth of synoviocytes from arthritic and normal joints: stimulation by exogenous platelet-derived growth factor and inhibition by transforming growth factor-beta and retinoids. J Clin Invest 1989;83:1267–76.
44. Bucala R, Ritchlin C, Winchester R, Cerami A. Constitutive production of inflammatory and mitogenic cytokines by rheumatoid synovial fibroblasts. J Exp Med 1991;173:569–74.
45. Remmers EF, Lafyatis R, Kumkumian GK, Case JP, Roberts AB, Sporn MB, et al. Cytokines and growth regulation of synoviocytes from patients with rheumatoid arthritis and rats with streptococcal cell wall arthritis. Growth Factors 1990;2:179–88.
46. Trabandt A, Gay RE, Gay S. Oncogene activation in rheumatoid synovium. Apmis 1992;100:861–75.
47. Roivainen A, Jalava J, Pirila L, Yli-Jama T, Tiusanen H, Toivanen P. H-ras oncogene point mutations in arthritic synovium. Arthritis Rheum 1997;40:1636–43.
48. Roivainen A, Isomaki P, Nikkari S, Saario R, Vuori K, Toivanen P. Oncogene expression in synovial fluid cells in reactive and early rheumatoid arthritis: a brief report. Br J Rheumatol 1995;34: 805–8.
49. Hashiramoto A, Sano H, Maekawa T, Kawahito Y, Kimura S, Kusaka Y, et al. C-myc antisense oligodeoxynucleotides can induce apoptosis and down-regulate Fas expression in rheumatoid synoviocytes. Arthritis Rheum 1999;42:954–62.
50. Dobrowolski S, Harter M, Stacey DW. Cellular ras activity is required for passage through multiple points of the G0/G1 phase in BALB/c 3T3 cells. Mol Cell Biol 1994;14:5441–9.
51. Karin M. Mitogen-activated protein kinase cascades as regulators of stress responses. Ann N Y Acad Sci 1998;851:139–46.
52. Lee JC, Laydon JT, McDonnell PC, Gallagher TF, Kumar S, Green D, et al. A protein kinase involved in the regulation of inflammatory cytokine biosynthesis. Nature 1994;372:739–46.
53. Schett G, Tohidast-Akrad M, Smolen JS, Schmid BJ, Steiner CW, Bitzan P, et al. Activation, differential localization, and regulation of the stress-activated protein kinases, extracellular signal-regulated kinase, c-Jun N-terminal kinase, and p38 mitogen-activated protein kinase, in synovial tissue and cells in rheumatoid arthritis. Arthritis Rheum 2000;43:2501–12.
54. Lomaga MA, Yeh WC, Sarosi I, Duncan GS, Furlonger C, Ho A, et al. TRAF6 deficiency results in osteopetrosis and defective interleukin-1, CD40, and LPS signaling. Genes Dev 1999;13: 1015–24.
55. Caunt CJ, Kiss-Toth E, Carlotti F, Chapman R, Qwarnstrom EE. Ras controls tumor necrosis factor receptor-associated factor (TRAF)6-dependent induction of nuclear factor-κB: selective regulation through receptor signaling components. J Biol Chem 2001;276:6280–8.
56. Naito A, Azuma S, Tanaka S, Miyazaki T, Takaki S, Takatsu K, et al. Severe osteopetrosis, defective interleukin-1 signalling and lymph node organogenesis in TRAF6-deficient mice. Genes Cells 1999;4:353–62.
57. McDermott EP, O'Neill LA. Ras participates in the activation of p38 MAPK by interleukin-1 by associating with IRAK, IRAK2, TRAF6, and TAK-1. J Biol Chem 2002;277:7808–15.
58. Houssiau FA, Devogelaer JP, Van Damme J, de Deuxchaisnes CN, Van Snick J. Interleukin-6 in synovial fluid and serum of patients with rheumatoid arthritis and other inflammatory arthritides. Arthritis Rheum 1988;31:784–8.
59. Brozik M, Rosztoczy I, Meretey K, Balint G, Gaal M, Balogh Z, et al. Interleukin 6 levels in synovial fluids of patients with different arthritides: correlation with local IgM rheumatoid factor and systemic acute phase protein production. J Rheumatol 1992;19: 63–8.
60. Kotake S, Sato K, Kim KJ, Takahashi N, Udagawa N, Nakamura I, et al. Interleukin-6 and soluble interleukin-6 receptors in the synovial fluids from rheumatoid arthritis patients are responsible for osteoclast-like cell formation. J Bone Miner Res 1996;11: 88–95.
61. Miyazawa K, Mori A, Yamamoto K, Okudaira H. Constitutive transcription of the human interleukin-6 gene by rheumatoid synoviocytes: spontaneous activation of NF-kappaB and CBF1. Am J Pathol 1998;152:793–803.
62. Ohshima S, Saeki Y, Mima T, Sasai M, Nishioka K, Nomura S, et al. Interleukin 6 plays a key role in the development of antigen-induced arthritis. Proc Natl Acad Sci U S A 1998;95:8222–6.
63. Takagi N, Mihara M, Moriya Y, Nishimoto N, Yoshizaki K, Kishimoto T, et al. Blockage of interleukin-6 receptor ameliorates joint disease in murine collagen-induced arthritis. Arthritis Rheum 1998;41:2117–21.
64. Miyazawa K, Mori A, Miyata H, Akahane M, Ajisawa Y, Okudaira H. Regulation of interleukin-1β-induced interleukin-6 gene expression in human fibroblast-like synoviocytes by p38 mitogen-activated protein kinase. J Biol Chem 1998;273:24832–8.
65. Miyazaki T, Katagiri H, Kanegae Y, Takayanagi H, Sawada Y, Yamamoto A, et al. Reciprocal role of ERK and NF-kappaB pathways in survival and activation of osteoclasts. J Cell Biol 2000;148:333–42.

Distinct roles of Smad pathways and p38 pathways in cartilage-specific gene expression in synovial fibroblasts

Hiroaki Seto,[1,2] Satoshi Kamekura,[1] Toshiki Miura,[1] Aiichiro Yamamoto,[1] Hirotaka Chikuda,[1] Toru Ogata,[1] Hisatada Hiraoka,[1] Hiromi Oda,[1] Kozo Nakamura,[1] Hisashi Kurosawa,[2] Ung-il Chug,[3] Hiroshi Kawaguchi,[1] and Sakae Tanaka[1]

[1]Department of Orthopaedic Surgery, Faculty of Medicine, The University of Tokyo, Tokyo, Japan. [2]Department of Orthopaedics, Juntendo University School of Medicine, Tokyo, Japan. [3]Division of Tissue Engineering, University of Tokyo Hospital, Tokyo, Japan.

The role of TGF-β/bone morphogenetic protein signaling in the chondrogenic differentiation of human synovial fibroblasts (SFs) was examined with the adenovirus vector-mediated gene transduction system. Expression of constitutively active activin receptor-like kinase 3 ($ALK3^{CA}$) induced chondrocyte-specific gene expression in SFs cultured in pellets or in SF pellets transplanted into nude mice, in which both the Smad and p38 pathways are essential. To analyze downstream cascades of ALK3 signaling, we utilized adenovirus vectors carrying either Smad1 to stimulate Smad pathways or constitutively active MKK6 ($MKK6^{CA}$) to activate p38 pathways. Smad1 expression had a synergistic effect on $ALK3^{CA}$, while activation of p38 MAP kinase pathways alone by transduction of $MKK6^{CA}$ accelerated terminal chondrocytic differentiation, leading to type X collagen expression and enhanced mineralization. Overexpression of Smad1 prevented $MKK6^{CA}$-induced type X collagen expression and maintained type II collagen expression. In a mouse model of osteoarthritis, activated p38 expression as well as type X collagen staining was detected in osteochondrophytes and marginal synovial cells. These results suggest that SFs can be differentiated into chondrocytes via ALK3 activation and that stimulating Smad pathways and controlling p38 activation at the proper level can be a good therapeutic strategy for maintaining the healthy joint homeostasis and treating degenerative joint disorders.

Introduction

Injury to the articular cartilage occurs under various pathological conditions such as trauma, inflammation, and aging (1), and cartilage injury is followed by osteoarthritic changes of the affected joints. Osteoarthritis is the most common degenerative joint disorder, affecting nearly half of the elderly population. Osteoarthritis is characterized by degradation of articular cartilage and overgrowth of cartilage and bone, known as osteophytes, at the periphery of the articular surface, which results in pain and loss of joint function (1, 2). Microscopically, loss of proteoglycan and fibrillation of the articular surface are observed at the early stage of arthritis. At later stages, clefts are formed, and at the end stage, erosive changes in the articular cartilage appear. The high prevalence of this disease results in high costs for treating patients, and therefore the development of good therapeutics for osteoarthritis is a matter of great urgency. Because of the limited capacity of spontaneous healing, the regeneration of intact articular cartilage is one of the most challenging issues in the orthopedic field (3, 4). Transplantation of autologous chondrocytes or mesenchymal progenitor cells and autogenous osteochondral transplantation (mosaicplasty) have been successfully utilized for the repair of focal osteochondral defects (3, 5–11). However, the application of these technologies is limited to small defects due to the difficulty of obtaining a sufficient amount of cells or tissues.

Synovium is a thin tissue lining the nonarticular surfaces of diarthrodial joints (12). Synovial tissues contain various types of cells, including type A cells, macrophage lineage cells, and type B cells, which are specialized synovial fibroblasts (SFs). It is now widely recognized that synovial tissues are involved primarily in the pathogenesis of arthritic joint disorders such as rheumatoid arthritis by producing the matrix-degenerating enzymes cystein proteases and matrix metalloproteinases (MMPs) and the proinflammatory cytokines interleukin-1 (IL-1) and tumor necrosis factor-α (TNF-α) (12). We previously reported that SFs express a high level of receptor activator of NF-κB ligand, the osteoclast differentiation factor belonging to the TNF-α superfamily (13). In contrast to such catabolic actions, there is accumulating evidence that synovial cells have anabolic effects, leading to bone and cartilage production. Hunziker and Rosenburg reported that synovial cells can migrate into partial-thickness articular cartilage defects, where they proliferate and subsequently deposit a scar-like tissue (14). Nishimura et al. (15) demonstrated SFs show chondrogenic differentiation after being cultured in the presence of TGF-β, and de Bari et al. recently demonstrated that multipotent mesenchymal stem cells could be isolated from human synovial tissues, which differentiated into chondrocytes as well as osteoblasts, adipocytes, and myotubes under proper culture conditions (16, 17). Another dramatic clinical manifestation of the chondrogenic potential of synovial tissues is synovial chondromatosis, a tumor-like disorder characterized by the formation of multiple cartilaginous nodules, which is believed to be benign reactive metaplasia of synovial cells (18). These observations

Nonstandard abbreviations used: anterior cruciate ligament (ACL); bone morphogenetic protein (BMP); constitutively active activin receptor-like kinase 3 ($ALK3^{CA}$); constitutively active MKK6 ($MKK6^{CA}$); hemagglutinin (HA); matrix metalloproteinase (MMP); medial meniscus (MM); osteoarthritis (OA); receptor-regulated Smad (R-Smad); synovial fibroblast (SF); TGF-β–activating kinase 1 (TAK1).

Conflict of interest: The authors have declared that no conflict of interest exists.

Citation for this article: *J. Clin. Invest.* 113:718–726 (2004). doi:10.1172/JCI200419899.